

# Output-sensitive Computation of Generalized Persistence Diagrams for 2-filtrations \*

Dmitriy Morozov<sup>1</sup> and Amit Patel<sup>2</sup>

<sup>1</sup>Lawrence Berkeley National Laboratory

<sup>2</sup>Department of Mathematics, Colorado State University

## Abstract

When persistence diagrams are formalized as the Möbius inversion of the birth–death function, they naturally generalize to the multi-parameter setting and enjoy many of the key properties, such as stability, that we expect in applications. The direct definition in the 2-parameter setting, and the corresponding brute-force algorithm to compute them, require  $\Omega(n^4)$  operations, where  $n$  is the complexity of the input. But the size of the generalized persistence diagram,  $C$ , can be as low as linear (and as high as cubic). We elucidate a connection between the 2-parameter and the ordinary 1-parameter settings, which allows us to design an output-sensitive algorithm, whose running time is in  $O(n^2m + Cm)$ , where  $m$  is the number of simplices in the input.

## 1 Introduction

An ordinary 1-parameter persistence diagram has a remarkable number of equivalent definitions: via persistent homology groups [13], as indecomposable summands of persistence modules [7, 32], via well groups [2] or persistence landscapes [6], and as the Möbius inversion of the rank invariant [26], to name a few. But extending these to the multi-parameter setting leads to very different objects with wildly different properties [8, 14, 20, 23, 31].

The latter definition, although implicitly recognized in the inclusion–exclusion formula used in the original proof of stability [10] and in size theory [15], received no attention until recently. Recognizing this formula as a special case of the Möbius inversion allows for generalizations in many directions. Kim and Mémoli were the first to apply the Möbius inversion to multiparameter persistence modules [20]. They define the persistence diagram

---

\*This work was supported by the Laboratory Directed Research and Development Program (LDRD) of Lawrence Berkeley National Laboratory under U.S. Department of Energy Contract No. DE-AC02-05CH11231 (DM). This work is partially funded by Leverhulme Trust grant VP2-2021-008 (AP).

as the Möbius inversion of the generalized rank invariant. We, however, are using a different definition. For us, the persistence diagram is the Möbius inversion of the birth–death function [17, 18], specifically, as defined by McCleary and Patel [23] and further generalized by Gülem and McCleary [16]. The most important property of this approach is that it is functorial. Functoriality plays a big role in justifying many of the choices we make in this paper. It is important to note there are other approaches to persistence using the Möbius inversion [1, 3, 5].

A question that remains open is how to efficiently compute the generalized persistence diagram. It is unclear how to take advantage of existing work. Computing indecomposable summands [12] doesn’t give a generalized persistence diagram, except in special cases for a different formulation [4]. Computing a minimal presentation of a module [19, 21] ought to help in general, although not in the specific setting described in this paper.

We consider the case of the 2-filtration. We assume that the underlying simplicial complex has  $m$  simplices, and the sum of the number of minimal grades at which the simplices appear — the amount of information needed to describe the filtration — is  $n \geq m$ . ( $n = m$  is the so-called 1-critical case.) It is possible to use the definition of the Möbius inversion directly as an algorithm (expressed below as Corollary 2.8). This formulation has  $16 \cdot n^4$  terms, and relies on the ability to compute the rank of any map between a pair of homology groups in the 2-filtration. An  $O(m^4)$  algorithm for the latter task in the 1-critical setting is given, for example, in [24, Section 4.4.2]; it can be readily adapted to the general setting. Together the two observations lead to an  $O(n^4)$  algorithm [4]. Unfortunately, because it has to examine all intervals in the 2-filtration, the algorithm is also in  $\Omega(n^4)$ .

On the other hand, a generalized persistence diagram can be very sparse. Its support, i.e., the number of non-zero intervals, can be as low as  $m$ , for example, if the 2-filtration is 1-critical and any monotone path gives the same ordering of simplices. We use  $C$  to denote the number of non-zero intervals, the size of the output in our problem.

Our contributions are two-fold. After recapping the necessary background in Sections 2 and 3, we establish a connection, in Section 4, between the non-zero intervals in the Möbius inversion and the pairing switches [11] between simplices along four paths through the 2-filtration. In Section 5, we develop an algorithm for computing the generalized persistence diagram that traverses the 2-filtration via a sequence of paths by performing transpositions of adjacent simplices. It maintains extended pairing information (that we call the *birth curves*), which allows us to compute all the intervals in the output-sensitive  $O(n^2m + Cm)$  time.

## 2 Background

### 2.1 Möbius inversion

Let  $P$  be any finite poset. For every pair of grades  $a, b \in P$ , the *interval*  $[a, b]$  is the subset  $\{x \in P : a \leq x \leq b\}$ . The set of all intervals  $\text{Int } P$  is a poset, where  $[a, b] \leq [c, d]$  whenever  $a \leq c$  and  $b \leq d$ . A *monotone function* between posets is a function  $f : P \rightarrow Q$  such that

for every  $\mathbf{a} \leq \mathbf{b}$  in  $\mathbf{P}$ ,  $f(\mathbf{a}) \leq f(\mathbf{b})$  in  $\mathbf{Q}$ . The operator  $\text{Int}$  takes  $f$  to a monotone function  $\text{Int } f : \text{Int } \mathbf{P} \rightarrow \text{Int } \mathbf{Q}$  where  $\text{Int } f[\mathbf{a}, \mathbf{b}] := [f(\mathbf{a}), f(\mathbf{b})]$ .

We are interested in the  $\mathbb{Z}$ -incidence algebra on  $\text{Int } \mathbf{P}$ , denoted  $\text{Inc}(\text{Int } \mathbf{P})$ . It is the set of all integral functions  $\alpha : \text{Int } \text{Int } \mathbf{P} \rightarrow \mathbb{Z}$  along with two binary operations:

$$\begin{aligned} (\alpha + \beta)([\mathbf{a}, \mathbf{b}], [\mathbf{c}, \mathbf{d}]) &:= \alpha([\mathbf{a}, \mathbf{b}], [\mathbf{c}, \mathbf{d}]) + \beta([\mathbf{a}, \mathbf{b}], [\mathbf{c}, \mathbf{d}]) \\ (\alpha * \beta)([\mathbf{a}, \mathbf{b}], [\mathbf{c}, \mathbf{d}]) &:= \sum_{[\mathbf{a}, \mathbf{b}] \leq [\mathbf{x}, \mathbf{y}] \leq [\mathbf{c}, \mathbf{d}]} \alpha([\mathbf{a}, \mathbf{b}], [\mathbf{x}, \mathbf{y}]) \cdot \beta([\mathbf{x}, \mathbf{y}], [\mathbf{c}, \mathbf{d}]). \end{aligned}$$

The additive identity is the *zero function*, and the multiplicative identity is the *delta function* defined as  $\delta([\mathbf{a}, \mathbf{b}], [\mathbf{c}, \mathbf{d}]) = 1$ , for  $[\mathbf{a}, \mathbf{b}] = [\mathbf{c}, \mathbf{d}]$ , and 0 otherwise. One may think of elements of  $\text{Inc}(\text{Int } \mathbf{P})$  as square matrices where both columns and rows are indexed by  $\text{Int } \mathbf{P}$ . Addition is matrix addition, and multiplication is matrix multiplication.

We are interested in two special functions in  $\text{Inc}(\text{Int } \mathbf{P})$ : the zeta function and the Möbius function. The *zeta function* is the function  $\zeta([\mathbf{a}, \mathbf{b}], [\mathbf{c}, \mathbf{d}]) = 1$ , for all  $[\mathbf{a}, \mathbf{b}] \leq [\mathbf{c}, \mathbf{d}]$ , and 0 otherwise. The zeta function is invertible and its (multiplicative) inverse, called the *Möbius function*  $\mu$ , can be described inductively as follows (see [29, Proposition 1]):

$$\mu([\mathbf{a}, \mathbf{b}], [\mathbf{c}, \mathbf{d}]) = \begin{cases} 1 & \text{for } [\mathbf{a}, \mathbf{b}] = [\mathbf{c}, \mathbf{d}] \\ - \sum_{[\mathbf{a}, \mathbf{b}] < [\mathbf{x}, \mathbf{y}] \leq [\mathbf{c}, \mathbf{d}]} \mu([\mathbf{x}, \mathbf{y}], [\mathbf{c}, \mathbf{d}]) & \text{for } [\mathbf{a}, \mathbf{b}] < [\mathbf{c}, \mathbf{d}] \\ 0 & \text{otherwise.} \end{cases} \quad (1)$$

Given a function  $f : \text{Int } \mathbf{P} \rightarrow \mathbb{Z}$ , there is a unique function  $g : \text{Int } \mathbf{P} \rightarrow \mathbb{Z}$  such that

$$f[\mathbf{c}, \mathbf{d}] = \sum_{[\mathbf{a}, \mathbf{b}] \leq [\mathbf{c}, \mathbf{d}]} g[\mathbf{a}, \mathbf{b}]. \quad (2)$$

This unique function  $g$  is called the *Möbius inversion* of  $f$  (see [29, Proposition 2]). It can be calculated as  $f$  convolved with the Möbius function  $\mu$  as follows:

$$g[\mathbf{c}, \mathbf{d}] = \sum_{[\mathbf{a}, \mathbf{b}] \leq [\mathbf{c}, \mathbf{d}]} f[\mathbf{a}, \mathbf{b}] \cdot \mu([\mathbf{a}, \mathbf{b}], [\mathbf{c}, \mathbf{d}]). \quad (3)$$

To recover  $f$  from  $g$ , convolve with the zeta function as follows:

$$\begin{aligned} \sum_{[\mathbf{a}, \mathbf{b}] \leq [\mathbf{c}, \mathbf{d}]} g[\mathbf{c}, \mathbf{d}] &= \sum_{[\mathbf{a}, \mathbf{b}] \leq [\mathbf{c}, \mathbf{d}]} g[\mathbf{a}, \mathbf{b}] \cdot \zeta([\mathbf{a}, \mathbf{b}], [\mathbf{c}, \mathbf{d}]) \\ &= \sum_{[\mathbf{a}, \mathbf{b}] \leq [\mathbf{c}, \mathbf{d}]} \left( \sum_{[\mathbf{x}, \mathbf{y}] \leq [\mathbf{a}, \mathbf{b}]} f[\mathbf{x}, \mathbf{y}] \cdot \mu([\mathbf{x}, \mathbf{y}], [\mathbf{a}, \mathbf{b}]) \right) \cdot \zeta([\mathbf{a}, \mathbf{b}], [\mathbf{c}, \mathbf{d}]) \\ &= \sum_{[\mathbf{x}, \mathbf{y}] \leq [\mathbf{c}, \mathbf{d}]} f[\mathbf{x}, \mathbf{y}] \cdot \left( \sum_{[\mathbf{x}, \mathbf{y}] \leq [\mathbf{a}, \mathbf{b}] \leq [\mathbf{c}, \mathbf{d}]} \mu([\mathbf{x}, \mathbf{y}], [\mathbf{a}, \mathbf{b}]) \cdot \zeta([\mathbf{a}, \mathbf{b}], [\mathbf{c}, \mathbf{d}]) \right) \\ &= \sum_{[\mathbf{x}, \mathbf{y}] \leq [\mathbf{c}, \mathbf{d}]} f[\mathbf{a}, \mathbf{b}] \cdot \delta([\mathbf{x}, \mathbf{y}], [\mathbf{c}, \mathbf{d}]) = f[\mathbf{c}, \mathbf{d}]. \end{aligned}$$

Thus, we interpret the convolution of  $f$  with  $\mu$  as the derivative of  $f$  and the convolution of  $g$  with  $\zeta$  as the integral of  $g$ .

## 2.2 Filtrations

We now describe the (generalized) persistence diagram of a filtration as the Möbius inversion of its birth–death function as defined in [23].

Let  $\mathcal{P}$  be a finite poset with a unique maximal element, denoted  $\top$ , and a unique minimal element, denoted  $\perp$ . Fix a finite simplicial complex  $K$ , and let  $\Delta K$  be the poset of all subcomplexes of  $K$  ordered by inclusion.

**Definition 2.1:** A  $\mathcal{P}$ -filtration of  $K$  is a monotone function  $F : \mathcal{P} \rightarrow \Delta K$  such that  $F(\perp) = \emptyset$  and  $F(\top) = K$ . Note that when  $\mathcal{P}$  is totally ordered, a simplex enters the filtration at a unique element of  $\mathcal{P}$ . For general  $\mathcal{P}$ , a simplex may enter at multiple incomparable grades of  $\mathcal{P}$ .

For each dimension  $d$ , denote by  $C_d(K)$  the  $k$ -vector space generated by the set of  $d$ -simplices in  $K$ . For every  $\mathbf{a} \in \mathcal{P}$ , let  $Z_d F(\mathbf{a}) \subseteq C_d(K)$  be the subspace of  $d$ -cycles in  $F(\mathbf{a})$  and let  $B_d F(\mathbf{a}) \subseteq C_d(K)$  be the subspace of  $d$ -boundaries in  $F(\mathbf{a})$ .

**Definition 2.2:** The  $d$ -th birth–death function of the  $\mathcal{P}$ -filtration  $F$  is the monotone integral function  $ZB_d F : \text{Int } \mathcal{P} \rightarrow \mathbb{Z}$  defined as follows:

$$ZB_d F[\mathbf{a}, \mathbf{b}] = \begin{cases} \dim(Z_d F(\mathbf{a}) \cap B_d F(\mathbf{b})) & \text{if } \mathbf{b} \neq \top \\ \dim Z_d F(\mathbf{a}) & \text{if } \mathbf{b} = \top. \end{cases}$$

The second case of  $\mathbf{b} = \top$  is necessary because it captures cycles that live forever. Without it, the persistence diagram of  $F$ , as defined below, will ignore all essential cycles of  $K$ .

**Definition 2.3:** The  $d$ -th persistence diagram of the  $\mathcal{P}$ -filtration  $F$  is the Möbius inversion, denoted  $\text{Dgm}_d F$ , of its the birth–death function  $ZB_d F$ .

We will suppress the dimension  $d$  in  $Z_d F$ ,  $B_d F$ ,  $ZB_d F$ , and  $\text{Dgm}_d F$  when it is of no importance.

**Remark 2.4:** The above idea for defining the  $d$ -th persistence diagram of a  $\mathcal{P}$ -filtration also works for any  $\mathcal{P}$ -module. That is, let  $M : \mathcal{P} \rightarrow \text{Vec}$  be a functor, i.e.,  $\mathcal{P}$ -module. Then there is a birth–death function associated to  $M$  and its persistence diagram is its Möbius inversion [16]. Further, the persistence diagram  $\text{Dgm}_d F$  of a  $\mathcal{P}$ -filtration  $F$ , as defined above, is the same, up to the diagonal, as the persistence diagram of the  $\mathcal{P}$ -module  $H_d F$  obtained by applying homology to the filtration [27].

## 2.3 Möbius Inversion for 1-Filtrations

We now study the familiar case of 1-filtrations, which are filtrations over totally ordered posets.

Let  $P_n$  be the totally ordered poset  $\{\perp = 0 < 1 < \dots < n = \top\}$ . The lemma below follows from Equation (1) by elementary calculations. See [30, Chapter 3.8] for a guide on how to compute Möbius functions.

**Lemma 2.5:** The Möbius function  $\mu \in \text{Inc}(\text{Int } P_n)$  is particularly nice. For every non-empty interval  $[c, d] \in \text{Int } P_n$ ,

$$\mu([a, b], [c, d]) = \begin{cases} (-1)^i \cdot (-1)^j & \text{if } \exists i, j \in \{0, 1\} \text{ such that } [a, b] = [c - i, d - j] \\ 0 & \text{otherwise} \end{cases}$$

The following corollary is an immediate consequence of Equation (3) and Lemma 2.5.

**Corollary 2.6:** Let  $F : P_n \rightarrow \Delta K$  be a 1-filtration and  $\text{Dgm}_d F$  its  $d$ -th persistence diagram. Then, for any interval  $[a, b] \in \text{Int } P_n$ ,

$$\text{Dgm}_d F[a, b] = \sum_{i, j \in \{0, 1\}} (-1)^i \cdot (-1)^j \cdot \text{ZB}_d F[a - i, b - j].$$

If the interval  $[a - i, b - j]$  does not exist, then we interpret  $\text{ZB}_d F[a - i, b - j]$  as zero.

## 2.4 Möbius Inversion for 2-Filtrations

We now consider 2-filtrations, which are filtrations over the product of two totally ordered posets and the main object of study in this paper.

Let  $L_n := P_n \times P_n$  be the product poset defined as follows. Its grades are tuples  $\mathbf{a} = (a_1, a_2)$ , and the partial ordering is  $\mathbf{a} = (a_1, a_2) \leq \mathbf{b} = (b_1, b_2)$  whenever  $a_1 \leq b_1$  and  $a_2 \leq b_2$ . The minimal element is  $\perp = (0, 0)$  and the maximal element is  $\top = (n, n)$ . The lemma below follows from Equation (1) by elementary calculations. See [30, Chapter 3.8] for a guide on how to compute Möbius functions.

**Lemma 2.7:** The Möbius function  $\mu \in \text{Inc}(\text{Int } L_n)$  is particularly nice. For every non-empty interval  $[c, d] \in \text{Int } L_n$ ,

$$\mu([a, b], [c, d]) = \begin{cases} (-1)^{\#i} \cdot (-1)^{\#j} & \text{if } \exists i, j \in \{0, 1\}^2 : [a, b] = [c - i, d - j] \\ 0 & \text{otherwise,} \end{cases}$$

where  $\#i := (i_1 + i_2) \bmod 2$  and similarly for  $\#j$ .

A *2-filtration* is a filtration  $F : L_n \rightarrow \Delta K$  indexed by the product of two totally ordered posets. The following corollary is an immediate consequence of Equation (3) and Lemma 2.7.

**Corollary 2.8:** Let  $F : L_n \rightarrow \Delta K$  be a 2-filtration and  $\text{Dgm}_d F$  its  $d$ -th persistence diagram. Then, for any interval  $[a, b] \in \text{Int } L_n$ ,

$$\text{Dgm}_d F[a, b] = \sum_{i, j \in \{0, 1\}^2} (-1)^{\#i} \cdot (-1)^{\#j} \cdot \text{ZB}_d F[a - i, b - j].$$

where  $\#i = (i_1 + i_2) \bmod 2$  and similarly for  $\#j$ . If the interval  $[a - i, b - j]$  does not exist, then we interpret  $\text{ZB}_d F[a - i, b - j]$  as zero.

## 2.5 Rota's Galois Connection Theorem

Functoriality of the (generalized) persistence diagram, as first observed in [23], plays an important role in justifying the seemingly arbitrary choices we make in this paper. The recent work of Gülem and McCleary [16] shows that functoriality of the persistence diagram is equivalent to Rota's Galois Connection Theorem. We now state their version of this theorem for persistence diagrams.

A (monotone) *Galois connection* from a poset  $P$  to a poset  $Q$ , written  $f : P \rightleftharpoons Q : g$ , are monotone functions  $f$  and  $g$  such that for all  $a \in P$  and  $x \in Q$ ,  $f(a) \leq x$  iff  $a \leq g(x)$ .

**Theorem 2.9** ([16]): Let  $F : P \rightarrow \Delta K$  and  $G : Q \rightarrow \Delta K$  be two filtrations and  $f : P \rightleftharpoons Q : g$  a Galois connection. If  $G = F \circ g$ , then for every  $x \leq y$  in  $Q$ ,

$$\text{Dgm}_d G[x, y] = \sum_{[a, b] \in (\text{Int } f)^{-1}[x, y]} \text{Dgm}_d F[a, b].$$

This theorem says that if two filtrations are related by a Galois connection, then the persistence diagram of one can be read from the other. Sections 2.6 to 2.8 make use of this theorem.

## 2.6 From 2-filtration to 1-filtrations

A 2-filtration over  $L_n$  induces a family of 1-filtrations when restricted to paths in  $L_n$ . We now apply Theorem 2.9 to study how their persistence diagrams relate.

**Definition 2.10:** A **step** in  $L_n$  is a pair of adjacent grades, i.e., grades that differ by 1 in a single position:  $(a, b) \rightarrow (a + 1, b)$ , or  $(a, b) \rightarrow (a, b + 1)$ . A **path** in  $L_n$  is a monotone sequence of  $2n$  steps starting at  $(0, 0)$  and ending at  $(n, n)$ . In other words, a path is a monotone, injective function  $p : P_{2n+1} \rightarrow L_n$ .

The path  $p$  induces a Galois connection  $f : L_n \rightleftharpoons P_{2n+1} : p$  as follows. For any  $a \in L_n$ , define  $f(a)$  as the unique minimal element  $x \in P_{2n+1}$  such that  $a \leq p(x)$ . Note  $f(a) \leq x$  iff  $a \leq p(x)$ . The following corollary follows from Theorem 2.9.

**Corollary 2.11:** Let  $F : L_n \rightarrow \Delta K$  be a 2-filtration and  $p : P_{2n+1} \rightarrow L_n$  a path. If  $G$  is the 1-filtration  $F \circ p : P_{2n+1} \rightarrow \Delta K$ , then for any  $x \leq y$  in  $P_{2n+1}$ ,

$$\text{Dgm}_d G[x, y] = \sum_{[a, b] \in (\text{Int } f)^{-1}[x, y]} \text{Dgm}_d F[a, b].$$

Here  $f$  comes from the Galois connection  $f : L_n \rightleftharpoons P_{2n+1} : p$  described above.

In other words, it is possible to read off the ordinary persistence diagram for any 1-filtration defined by a path through the poset  $L_n$  from the generalized persistence diagram of the 2-filtration. In this paper, we develop an algorithm that does the opposite. We glue the persistence diagrams for a family of paths into the persistence diagram of the 2-filtration.

## 2.7 Coarsening and refining

We now apply Theorem 2.9 to study how the persistence diagram of a filtration changes under refinement.

Refine  $P_n$  by dividing every step into multiple steps:

$$P_{n'} := \{0 < \dots < 1 < \dots < n-1 < \dots < n\}.$$

The product  $L_{n'} := P_{n'} \times P_{n'}$  is a refinement of  $L_n$ , and the two are related by a Galois connection  $f : L_{n'} \rightleftharpoons L_n : g$  as follows. For any  $(\mathbf{a}, \mathbf{b}) \in L_{n'}$ ,  $f(\mathbf{a}, \mathbf{b}) := ([\mathbf{a}], [\mathbf{b}])$ , and  $g$  is inclusion. The following corollary follows from Theorem 2.9.

**Corollary 2.12:** Let  $F : L_{n'} \rightarrow \Delta K$  and  $G : L_n \rightarrow \Delta K$  be filtrations and  $f : L_{n'} \rightleftharpoons L_n : g$  the Galois connection described above. If  $G = F \circ g$ , then for any  $x \leq y$  in  $G$ ,

$$\text{Dgm}_d G[x, y] = \sum_{[\mathbf{a}, \mathbf{b}] \in (\text{Int } f)^{-1}[x, y]} \text{Dgm}_d F[\mathbf{a}, \mathbf{b}].$$

This corollary highlights a significant advantage of generalized persistence diagrams: they are stable under refinement. Lack of this property is one of the chief problems with using indecomposable summands to generalize persistence diagrams (breaking ties in the input can significantly change the decomposition). Our definition of a 2-filtration allows two simplices to enter at the same grade. However, our algorithm does not. In this case, Corollary 2.12 enables us to break ties arbitrarily; see Section 3.

## 2.8 Birth–death vs rank functions

We now explain our preference for the birth–death function over the better-known rank function associated to a filtration.

Consider the classical definition of the persistence diagram associated to a 1-filtration  $G : P_n \rightarrow \Delta K$ . The  $d$ -th rank function associated to  $G$  is the function  $\text{rk}_d : \text{Int } P_n \rightarrow \mathbb{Z}$  that assigns to every interval  $[\mathbf{a}, \mathbf{b}]$  the rank of the linear map on homology  $H_d(G(\mathbf{a})) \rightarrow H_d(G(\mathbf{b}))$  induced by the inclusion  $G(\mathbf{a}) \hookrightarrow G(\mathbf{b})$ . The  $d$ -th persistence diagram of  $F$  is defined as the assignment to every  $\mathbf{a} < \mathbf{b}$  (up to a shift), the integer

$$\text{rk}_d[\mathbf{a}, \mathbf{b}] - \text{rk}_d[\mathbf{a} - 1, \mathbf{b}] + \text{rk}_d[\mathbf{a} - 1, \mathbf{b} + 1] - \text{rk}_d[\mathbf{a}, \mathbf{b} + 1].$$

This assignment can be interpreted as the Möbius inversion of  $\text{rk}_d F$  using the containment  $\supseteq$  relation on  $\text{Int } P_n$  instead of the product ordering we are using in this paper. That is,  $[c, d] \supseteq [a, b]$  if  $c \leq a$  and  $b \leq d$ .

We prefer the birth–death function over the rank function because it behaves well with Galois connections. Consider a Galois connection between arbitrary posets  $f : P \rightleftharpoons Q : g$  and apply  $\text{Int}$ . Assuming the product ordering on the two interval posets  $\text{Int } P$  and  $\text{Int } Q$ , we see

$$\text{Int } f[\mathbf{a}, \mathbf{b}] \leq [x, y] \text{ iff } [\mathbf{a}, \mathbf{b}] \leq \text{Int } g[x, y] \Leftrightarrow f(\mathbf{a}) \leq x \text{ and } f(\mathbf{b}) \leq y \text{ iff } \mathbf{a} \leq g(x) \text{ and } \mathbf{b} \leq g(y).$$



In other words,  $\text{Int } f : \text{Int } P \rightleftharpoons \text{Int } Q : \text{Int } g$  is a Galois connection. This observation is at the heart of the proof of Theorem 2.9. Unfortunately,  $\text{Int } f : \text{Int } P \rightleftharpoons \text{Int } Q : \text{Int } g$  fails to be a Galois connection under the containment ordering on  $\text{Int } P$  and  $\text{Int } Q$ . This makes Theorem 2.9 unavailable when using the rank function. We need Corollaries 2.11 and 2.12 to justify the choices we make later in this paper.

We prefer the birth–death function both for its theoretical properties and for the simpler interpretation of its Möbius inversion<sup>1</sup>. But we also note that because the two produce the same persistence diagram for the 1-filtrations, the algorithm described in this paper can be immediately adapted to computing the Möbius inversion of the rank function on the 2-filtration; only the output values have to be changed.

## 2.9 Transpositions

Fix a 1-filtration  $F : P_n \rightarrow \Delta K$  and assume that for every adjacent pair of subcomplexes, the difference  $F(i) - F(i - 1)$  is empty or a single simplex, denoted  $\sigma_i$ . Given the boundary matrix  $D$  of  $K$ , with rows and columns ordered by the 1-filtration, the standard persistence algorithm [13] finds a factorization [11],  $R = DV$ , where  $R$  is *reduced*, meaning the lowest non-zero entries in its columns appear in unique rows, and  $V$  is invertible upper-triangular. The lowest non-zeros in matrix  $R$  give the persistence pairing: for  $j \neq n$ ,  $\text{Dgm}[i, j] = 1$  iff  $R[i, j] \neq 0$  and  $R[i', j] = 0 \forall i' > i$ ; for  $j = n$ ,  $\text{Dgm}[i, n]$  is the number of zero columns  $i$  (such that  $R[\cdot, i]$  is 0) minus the number of non-zero columns  $j$  (such that  $\exists i, R[i, j] \neq 0$ ).

**Definition 2.13:** Whenever  $\text{Dgm}[i, j] \neq 0$ , we say  $\sigma_i$  is **paired** with  $\sigma_j$  and that  $\sigma_i$  is **positive** and  $\sigma_j$  is **negative**. Two pairs  $(\sigma_i, \sigma_j)$  and  $(\tau_k, \tau_l)$  are **nested** if the interval  $[i, j]$  is contained in the interval  $[k, l]$ . They are **disjoint** if  $[i, j] \cap [k, l] = \emptyset$ .

Cohen-Steiner et al. [11] (see also [24]) study what happens to the pairing when we transpose two simplices in the 1-filtration  $F$ . They analyze how the decomposition  $R = DV$  may fail to satisfy the requirement that  $R$  is reduced and  $V$  is invertible upper-triangular, and show that this property can be restored, following a single transposition, in linear time. Appendix A briefly recaps the details of the updates. The following lemma is a consequence of their analysis.

**Lemma 2.14** (Nested-Disjoint Lemma [11, 24]): The pairing of two transposing simplices can switch only if before the transposition their pairing is either nested, or disjoint. (If the switch occurs, the pairing remains nested or disjoint after the transposition.)

The contrapositive of this statement is an important shortcut that we use below: if the pairing of two transposing simplices is neither nested, nor disjoint, it will not change after the transposition.

---

<sup>1</sup>Suppose  $F$  is a 1-filtration, with  $i$  the minimal grade of simplex  $\sigma_i$ . Define a 2-filtration  $G$  so that the unique minimal grade of  $\sigma_i$  is  $(i, i)$ . The Möbius inversion of the birth–death function of  $G$  is  $\text{Dgm}G[(i, i), (j, j)] = +1$  if  $\text{Dgm}F[i, j] = +1$  and 0 otherwise. The Möbius inversion of the rank function on the other hand has values,  $\text{Dgm}^{\text{rk}}G[(i, i), (j, n)] = +1$ ,  $\text{Dgm}^{\text{rk}}G[(i, i), (n, j)] = +1$ ,  $\text{Dgm}^{\text{rk}}G[(i, i), (j, j)] = -1$  for every  $\text{Dgm}F[i, j] = +1$ .



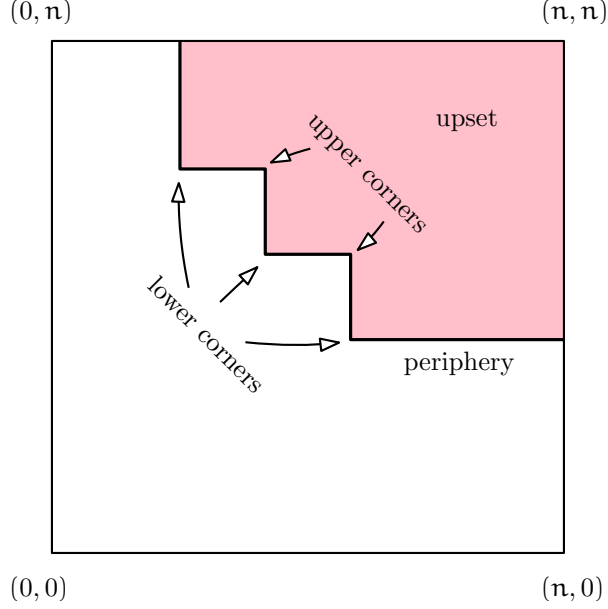


Figure 1: An upset in pink, its lower and upper corners, and periphery in bold.

### 3 Preliminaries

We now develop notation specializing to 2-filtrations and state an important lemma.

An *antichain* in  $L_n$  is any subset such that no two grades are comparable. An *upset* is a subset  $\mathbf{U} \subseteq L_n$  such that if  $\mathbf{a} \in \mathbf{U}$  and  $\mathbf{a} \leq \mathbf{b}$ , then  $\mathbf{b} \in \mathbf{U}$ . Since  $L_n$  is finite, its set of antichains is in bijection with its set of upsets. Fix an upset  $\mathbf{U}$ . A *lower corner* of  $\mathbf{U}$  is any minimal grade of  $\mathbf{U}$ . Note that the set of all lower corners of  $\mathbf{U}$  is an antichain; we denote it  $\text{lower}(\mathbf{U})$ . We say  $(i, j) \in \mathbf{U}$  is an *upper corner* of  $\mathbf{U}$  if  $(i-1, j)$  and  $(i, j-1)$  are in  $\mathbf{U}$  but  $(i-1, j-1)$  is not in  $\mathbf{U}$ . We denote the set of all upper corners as  $\text{upper}(\mathbf{U})$ . A *periphery* of  $\mathbf{U}$  is the set of grades  $(i, j)$  such that grades  $(i-1, j-1)$  are not in the upset. See Figure 1. (The periphery uniquely determines the upset, so we abuse the terminology and also refer to lower and upper corners of a periphery.)

Fix a 2-filtration  $F : L_n \rightarrow \Delta\mathbf{K}$ . For any simplex  $\sigma \in \mathbf{K}$ , let  $f(\sigma)$  denote the periphery of the upset  $\mathbf{U}_\sigma$  that contains  $\sigma$ . We call this the *appearance curve* of  $\sigma$ . Note that a path in  $L_n$  enters upset  $\mathbf{U}_\sigma$  at a unique grade of the appearance curve.

**Definition 3.1:** The 2-filtration  $F$  is **non-degenerate** if no two lower corners of any appearance curves share a component of a grade. That is, if  $(\mathbf{a}_1, \mathbf{a}_2)$  is a lower corner of  $f(\sigma)$  and  $(\mathbf{b}_1, \mathbf{b}_2)$  is a lower corner of  $f(\tau)$ , then  $\mathbf{a}_1 \neq \mathbf{b}_1$  and  $\mathbf{a}_2 \neq \mathbf{b}_2$ .

Every degenerate filtration  $F$  can be refined into a non-degenerate filtration  $G$  as follows. Consider a refinement  $L_{n'}$  of  $L_n$  and recall the Galois connection  $f : L_{n'} \rightleftarrows L_n : g$  from Section 2.7. Assuming  $L_{n'}$  is sufficiently fine, there is a non-degenerate filtration  $G : L_{n'} \rightarrow \Delta\mathbf{K}$  such that  $G = F \circ g$ , with ties in  $F$  broken arbitrarily, respecting the dimension of the simplices. Corollary 2.12 provides the equation for recovering  $\text{Dgm}F$  from  $\text{Dgm}G$ .

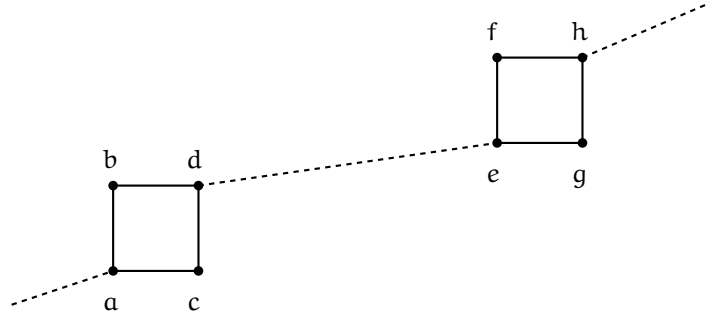


Figure 2: 1-dimensional paths through the 2-filtration involved in the analysis.

Throughout the paper, we use  $m = |\mathbf{K}|$  to denote the size of the simplicial complex, and  $n = \sum_{\sigma} |\text{lower}(f(\sigma))|$ , the complexity of the input, i.e., the size of the description of the minimal grades at which the simplices appear.

**Lemma 3.2** (Path Invariance): Let  $F : L_n \rightarrow \Delta\mathbf{K}$  be a non-degenerate filtration and  $\mathbf{p} : P_{2n+1} \rightarrow L_n$  any path. If simplex  $\sigma$  is added to the 1-filtration  $F \circ \mathbf{p}$  at step  $(i, j) \rightarrow (i + \delta_i, j + \delta_j)$ , simplex  $\tau$  is added to the 1-filtration at step  $(k, l) \rightarrow (k + \delta_k, l + \delta_l)$ , and  $\sigma$  and  $\tau$  are paired in the 1-filtration, then they are paired in every 1-filtration induced by any path taking these two steps.

*Proof.* Let  $K_1$  denote the complex  $F(i, j)$ ,  $K_2 = K_1 \cup \{\sigma\}$  denote the complex  $F(i + \delta_i, j + \delta_j)$ ,  $K_3$  denote the complex  $F(k, l)$ ,  $K_4 = K_3 \cup \{\tau\}$  denote the complex  $F(k + \delta_k, l + \delta_l)$ . Then the 1-filtration induced by any path taking these two steps contains the following 2-step filtration as a subfiltration:  $K_1 \subseteq K_2 \subseteq K_3 \subseteq K_4$ . From Corollary 2.6,  $\sigma$  and  $\tau$  are paired iff

$$\dim(\mathbf{Z}K_2 \cap \mathbf{B}K_4) - \dim(\mathbf{Z}K_1 \cap \mathbf{B}K_4) - \dim(\mathbf{Z}K_2 \cap \mathbf{B}K_3) + \dim(\mathbf{Z}K_1 \cap \mathbf{B}K_3) = 1.$$

In other words, the pairing is independent of the order of simplices in  $K_1$  and  $K_3 - K_2$ .  $\square$

## 4 Möbius Inversion from Transpositions

Fix a non-degenerate filtration  $F : L_n \rightarrow \Delta\mathbf{K}$ . To compute the persistence diagram  $\text{Dgm}F$  at the interval  $[d, h]$ , it suffices, by Corollary 2.8, to consider any four 1-dimensional paths through the 2-filtration that go through the subcomplexes  $F(d-i)$  and  $F(h-j)$  for  $i, j \in \{0, 1\}^2$ . We denote the four grades around  $d$  as  $a, b, c, d$  and the four grades around  $h$  as  $e, f, g, h$ ; see Figure 2. The four paths in question are:

$$\begin{array}{ccc} \dots abd \dots efh \dots & \leftrightarrow & \dots abd \dots egh \dots \\ & \updownarrow & \\ \dots acd \dots efh \dots & \leftrightarrow & \dots acd \dots egh \dots \end{array} \quad (4)$$

Because the filtration is non-degenerate, at most a single simplex appears at every one of the eight steps on these paths. Moreover, the only way two different simplices  $\sigma$  and  $\tau$  can

appear going from  $\mathbf{a}$  to  $\mathbf{d}$  (or from  $\mathbf{e}$  to  $\mathbf{h}$ ) is if  $\mathbf{d}$  is a minimum of the intersection of upsets of the appearance curves of  $\sigma$  and  $\tau$ . In this case, going between any two paths connected by an arrow results in a transposition of the two simplices in the 1-dimensional filtrations induced by the paths.

**2D from 1D.** For any two nested spaces  $F(\mathbf{x}) \subseteq F(\mathbf{y})$ , let  $\mathbf{xy}$  denote the value of the birth–death function  $\mathbf{ZBF}[\mathbf{x}, \mathbf{y}]$ . For any filtration

$$F(\mathbf{w}) \subseteq F(\mathbf{x}) \subseteq F(\mathbf{y}) \subseteq F(\mathbf{z}),$$

let  $\mathbf{wxyz}$  be the value of the 1-dimensional Möbius inversion of the birth–death function for the interval  $[\mathbf{x}, \mathbf{z}]$  in this filtration, namely

$$\mathbf{wxyz} = \mathbf{xz} - \mathbf{xy} - \mathbf{wz} + \mathbf{wy}. \quad (5)$$

With this notation, the 2-dimensional Möbius inversion can be rewritten in terms of the 1-dimensional Möbius inversions:

**Lemma 4.1:**

$$\mathbf{DgmF}[\mathbf{d}, \mathbf{h}] = (\mathbf{cdfh} - \mathbf{abfh}) - (\mathbf{cdeg} - \mathbf{abeg}) \quad (6)$$

$$= (\mathbf{cdgh} - \mathbf{abgh}) - (\mathbf{cdef} - \mathbf{abef}) \quad (7)$$

$$= (\mathbf{bdfh} - \mathbf{acfh}) - (\mathbf{bdeg} - \mathbf{aceg}) \quad (8)$$

$$= (\mathbf{bdgh} - \mathbf{acgh}) - (\mathbf{bdef} - \mathbf{acef}) \quad (9)$$

$$= \mathbf{adeh} - \mathbf{adef} - \mathbf{adeg} - \mathbf{abeh} - \mathbf{aceh} + \mathbf{abef} + \mathbf{abeg} + \mathbf{acef} + \mathbf{aceg}. \quad (10)$$

*Proof.* Expanding any one of the five formulae using Equation (5) results in

$$(\mathbf{dh} - \mathbf{df} - \mathbf{dg} + \mathbf{de}) - (\mathbf{ch} - \mathbf{cf} - \mathbf{cg} + \mathbf{ce}) - (\mathbf{bh} - \mathbf{bf} - \mathbf{bg} + \mathbf{be}) + (\mathbf{ah} - \mathbf{af} - \mathbf{ag} + \mathbf{ae}),$$

which equals  $\mathbf{DgmF}[\mathbf{d}, \mathbf{h}]$  by Corollary 2.8.  $\square$

If two different simplices,  $\sigma$  and  $\tau$ , appear as we go from  $\mathbf{a}$  to  $\mathbf{d}$  (or from  $\mathbf{e}$  to  $\mathbf{h}$ ) and their pairing does not switch, after a transposition, along any path through the bifiltration, then the value of the diagram  $\mathbf{DgmF}[\mathbf{d}, \cdot]$  (or  $\mathbf{DgmF}[\cdot, \mathbf{h}]$ ) is 0.

**Lemma 4.2:** Suppose  $F(\mathbf{x} - (1, 1)) - F(\mathbf{x}) = \{\sigma, \tau\}$ . Let  $\mathbf{p}_1$  and  $\mathbf{p}_2$  be two paths that both pass through grades  $\mathbf{x} - (1, 1)$  and  $\mathbf{x}$  and only differ in the step they take in between those grades. If for any such two paths, the pairing of simplices  $\sigma$  and  $\tau$  does not switch, then

$$\mathbf{DgmF}[\mathbf{x}, \cdot] = 0 \quad \text{and} \quad \mathbf{DgmF}[\cdot, \mathbf{x}] = 0.$$

*Proof.* We prove the first claim,  $\mathbf{DgmF}[\mathbf{x}, \cdot] = 0$ ; the second claim is proved analogously. Suppose  $\mathbf{x} = \mathbf{d} = (\mathbf{d}_1, \mathbf{d}_2)$  and assume, without loss of generality, that the appearance curve of  $\sigma$  has a lower-corner  $(\cdot, \mathbf{d}_2)$ , and the appearance curve of  $\tau$  has a lower-corner  $(\mathbf{d}_1, \cdot)$ . From

the 1-dimensional case, we know that if for any two paths going through  $\mathbf{a}$  and  $\mathbf{d}$ , simplex  $\sigma$  has the same pairing, then for any step  $\mathbf{x} \rightarrow \mathbf{y}$ , we have:

$$\mathbf{abxy} = \mathbf{cdxy} \quad \text{and} \quad \mathbf{xyab} = \mathbf{xycd},$$

depending whether  $\mathbf{d} \leq \mathbf{x}$  or  $\mathbf{y} \leq \mathbf{a}$ .

Taking  $\mathbf{x}, \mathbf{y}$  to be either  $\mathbf{f}, \mathbf{h}$  or  $\mathbf{e}, \mathbf{g}$ , we get:

$$\begin{aligned} 0 &= (\mathbf{cdfh} - \mathbf{abfh}) - (\mathbf{cdeg} - \mathbf{abeg}) \\ &= \text{DgmF}[\mathbf{d}, \mathbf{h}]. \end{aligned} \quad (\text{By Equation (6) in Lemma 4.1.})$$

□

**Three cases.** Because  $F$  is non-degenerate, there are at most two persistence pairs between  $\mathbf{d}$  and  $\mathbf{h}$  in the filtration  $F(\mathbf{a}) \subseteq F(\mathbf{d}) \subseteq F(\mathbf{e}) \subseteq F(\mathbf{h})$ .

**Lemma 4.3:** If  $F$  is non-degenerate, then  $\mathbf{adeh} \in \{0, 1, 2\}$ .

*Proof.* Because the filtration is non-degenerate, at most one simplex appears at any step around each one of the squares, and therefore at most two simplices appear between  $F(\mathbf{a})$  and  $F(\mathbf{d})$  as well as between  $F(\mathbf{e})$  and  $F(\mathbf{h})$ . It follows that at most two classes can be born between  $\mathbf{a}$  and  $\mathbf{d}$  and die between  $\mathbf{e}$  and  $\mathbf{h}$ . □

We now analyze the three possible values of  $\mathbf{adeh}$  separately.

## 4.1 No Pairs

If there are no 1-dimensional persistence pairs between  $\mathbf{d}$  and  $\mathbf{h}$ , then the value of the 2-dimensional diagram is zero.

**Theorem 4.4:** If  $\mathbf{adeh} = 0$ , then  $\text{DgmF}[\mathbf{d}, \mathbf{h}] = 0$ .

*Proof.* If  $\mathbf{adeh} = 0$ , then every one of the terms on the right-hand side of Equation (10) in Lemma 4.1 are also zero. (If any one of them was positive, it would contribute to a pair between  $\mathbf{d}$  and  $\mathbf{h}$  in the coarser filtration.) □

## 4.2 Single Pair

If there is one 1-dimensional pair between  $\mathbf{d}$  and  $\mathbf{h}$ , then the value of the 2-dimensional diagram has a simple expression. (This is a crucial result for our algorithm; we spell out its implications after the proof.)

**Theorem 4.5:** If  $\mathbf{adeh} = 1$ , then the value of the 2-dimensional diagram is given by

$$\text{DgmF}[\mathbf{d}, \mathbf{h}] = \mathbf{B} \cdot \mathbf{D},$$

where

$$\begin{aligned} B &= 1 - abeh - aceh \\ D &= 1 - adef - adeg. \end{aligned}$$

To prove this theorem, we need a set of auxiliary formulae.

**Proposition 4.6:** If  $adeh = 1$ , then

$$\begin{aligned} abeh \cdot adef &= abef \\ aceh \cdot adef &= acef \\ abeh \cdot adeg &= abeg \\ aceh \cdot adeg &= aceg. \end{aligned}$$

*Proof.* We prove the first statement by considering the 1-dimensional filtration

$$F(\mathbf{a}) \subseteq F(\mathbf{b}) \subseteq F(\mathbf{d}) \subseteq F(\mathbf{e}) \subseteq F(\mathbf{f}) \subseteq F(\mathbf{h}).$$

The right-hand side of the first statement is 1 iff a class born at  $\mathbf{b}$  dies at  $\mathbf{f}$ . Under the assumption  $adeh = 1$ , consider the class that is born between  $\mathbf{a}$  and  $\mathbf{d}$  and dies between  $\mathbf{e}$  and  $\mathbf{h}$ :

1. this class is born at  $\mathbf{b}$  iff  $abeh = 1$  (otherwise, it is born at  $\mathbf{d}$ ).
2. this class dies at  $\mathbf{f}$  iff  $adef = 1$  (otherwise, it dies at  $\mathbf{h}$ ).

It follows that if  $adeh = 1$ , then  $abeh \cdot adef = abef$ .

The other three statements are proved analogously. □

*Proof of Theorem 4.5.*

$$\begin{aligned} B \cdot D &= (1 - abeh - aceh) \cdot (1 - adef - adeg) \\ &= 1 - adef - adeg - abeh - aceh + \\ &\quad abeh \cdot adef + abeh \cdot adeg + aceh \cdot adef + aceh \cdot adeg \\ &= 1 - adef - adeg - abeh - aceh + \\ &\quad abef + abeg + acef + aceg \quad \text{(By Proposition 4.6.)} \\ &= adeh - adef - adeg - abeh - aceh + \quad \text{(By assumption } adeh = 1.) \\ &\quad abef + abeg + acef + aceg \\ &= \text{DgmF}[\mathbf{d}, \mathbf{h}]. \quad \text{(By Equation (10) in Lemma 4.1.)} \end{aligned}$$

□

**Implications.** To understand the algorithmic implications of Theorem 4.5, we need to dissect the terms  $B$  and  $D$ . Because the terms on the right-hand side of  $B = 1 - abeh - aceh$ , involve only a single step ( $a \rightarrow b$  or  $a \rightarrow c$ ) through the non-degenerate bifiltration, their values can be only 0 or 1. Accordingly,  $B$  can take on values  $-1, 0, 1$ .

- $B = -1$  iff both  $abeh$  and  $aceh$  are 1. This happens iff the class that dies between  $e$  and  $h$  is born along the steps  $a \rightarrow b$  and  $a \rightarrow c$  around the first square. If the same simplex appears at both steps, it means that  $d$  is the upper-corner of its appearance curve. If two different simplices appear, it means that the pairing switches when we transpose them in the filtration and that the first-to-appear simplex creates the class that dies between  $e$  and  $h$ .
- $B = 0$  iff only one of the two terms,  $abeh$  or  $aceh$ , is 1. Without loss of generality, suppose  $abeh = 1$ . Then, because a class that dies between  $e$  and  $h$  has to be born between  $a$  and  $d$ ,  $cdeh = 1$ . This cannot happen if the same simplex appears at steps  $a \rightarrow b$  and  $a \rightarrow c$  (otherwise, we'd get a contradiction with Lemma 3.2). If two different simplices appear at those steps, then the pairing does not switch when we transpose them.
- $B = 1$  iff both of the two terms,  $abeh$  and  $aceh$  are 0. In this case, the class that dies between  $e$  and  $h$  must be born along the steps  $b \rightarrow d$  and  $c \rightarrow d$  (which means  $bdeh = cdeh = 1$ ). This is possible if  $d$  is the lower corner of the appearance curve of a simplex. It is also possible for two different simplices to appear at the two steps (this happens if  $d$  is a minimum of the intersection of upsets of their appearance curves). In this case, the pairing switches after their transposition, and the simplex that appears last is the one that creates the dying class.

Similar analysis applies to the term  $D = 1 - adef - adeg$ .

- $D = -1$  iff the class born between  $a$  and  $d$  dies at the first step ( $e \rightarrow f$  and  $e \rightarrow g$ ) around the second square. This happens if the same simplex appears at the two steps, and  $h$  is the upper-corner of its appearance curve; or if two different simplices appear, the pairing switches when their order is transposed, with the first-to-appear simplex involved in the pair.
- $D = 0$  iff the class dies at the first step or at the second step, depending on which way we go around the square. This happens if the pairing does not switch as we change how we go around the square.
- $D = 1$  iff the class dies at the second step ( $f \rightarrow h$  and  $g \rightarrow h$ ) around the second square. This happens if  $h$  is a lower-corner in the appearance curve of a simplex, or if two different simplices appear and their pairing switches when they are transposed, with the last-to-appear simplex involved in the pair.

What is crucial for the algorithm in Section 5 is that for the terms  $B$  or  $D$  to be non-zero, the respective squares must go around either the lower-, or the upper-corner of the

appearance curve of the same simplex, or if two different simplices appear in the square, their pairing must switch, when we transpose them in the filtration. (The latter case is consistent with Lemma 4.2, but more precise. It tells us not only that some value in the diagram might be non-zero, but also narrows down the locations of the generalized pairs.)

### 4.3 Two Pairs

If  $\text{adeh} = 2$ , then two pairs of simplices,  $\sigma_1, \sigma_2$  and  $\tau_1, \tau_2$  appear in the first and in the second squares.

Consider the four paths around the two squares, see (4), and consider what happens to the pairing of the four simplices.

- If the pairing never switches, then  $\text{DgmF}[\mathbf{d}, \mathbf{h}] = 0$  by Lemma 4.2.
- If the pairing switches at least once, but doesn't switch everywhere, then along one of the paths the pairing has to be neither nested, nor disjoint (i.e., first simplex of  $\sigma_1, \sigma_2$  is paired with the first simplex of  $\tau_1, \tau_2$ , and second is paired with second). Without loss of generality, suppose we get such a pairing along the path  $\dots \mathbf{abd} \dots \mathbf{efh} \dots$ . Lemma 2.14 implies that no pairing switch is possible as we move to paths  $\dots \mathbf{acd} \dots \mathbf{efh} \dots$  and  $\dots \mathbf{abd} \dots \mathbf{egh} \dots$ . It follows that the two pairings of the simplices along those two paths is nested. Since we assumed that at least one switch in pairing occurs, it follows that the pairing switches as we take either one of the two transitions to path  $\dots \mathbf{acd} \dots \mathbf{egh} \dots$ , and in particular the pairs are nested. Using these four facts, implies

$$\begin{aligned} \mathbf{bdfh} &= 1 \\ \mathbf{acfh} &= 1 \\ \mathbf{bdeg} &= 1 \\ \mathbf{aceg} &= 0. \end{aligned}$$

Substituting the four terms into Equation (8), we get  $\text{DgmF}[\mathbf{d}, \mathbf{h}] = -1$ .

- If the pairing switches on each one of the four transpositions, then from Lemma 2.14, it follows that the first simplex to appear of  $\sigma_1$  and  $\sigma_2$  is paired with the last simplex to appear of  $\tau_1$  and  $\tau_2$  (and vice versa, last-to-appear is paired with the first-to-appear). In this case, we can use any one of the Equations (6) to (9) to get  $\text{DgmF}[\mathbf{d}, \mathbf{h}] = -2$ . We note that this case occurs generically (more on that in the next section).

## 5 Algorithm

We use the observations in the previous section to devise an algorithm that tracks the changes in pairing along 1-dimensional paths through the 2-filtration and identifies all intervals in the support of the generalized persistence diagram; its high-level overview is in Appendix B.



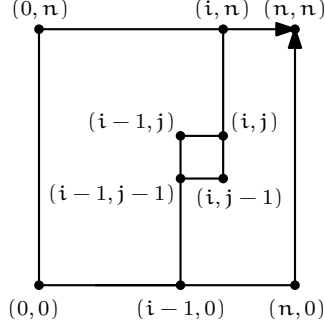


Figure 3: Path traversal starts with the path along the left and top edges of the 2-filtration, and through a sequence of elementary steps (one of which around  $(i, j)$  is shown in the figure) reaches the path along the bottom and right edge of the 2-filtration.

**Birth curves.** Suppose step  $(k - \delta_k, l - \delta_l) \rightarrow (k, l)$  in the 2-filtration adds a *negative* simplex  $\tau$ . Then the *birth curve* of  $\tau$  at this step is a periphery  $\mathbf{c}$  such that if a path  $\mathbf{p}$  through this step enters the periphery at step  $(i - \delta_i, j - \delta_j) \rightarrow (i, j)$ , then the simplex  $\sigma$  added along  $\mathbf{p}$  at this  $(i + j)$ -th step is paired with  $\tau$  in the 1-dimensional filtration induced by the path. Lemma 3.2 implies that birth curves are well-defined: if  $\sigma$  and  $\tau$  are paired along one path through the two steps, then they are paired along every path through them.

Our algorithm sweeps the 2-filtration and tracks birth curves of negative simplices. Recall from Section 3 that for each birth curve, its *lower corners* are the minimal grades in its upset; its *upper corners* are grades  $(i, j)$  in the upset, such that  $(i - 1, j)$  and  $(i, j - 1)$  are also in the upset, but  $(i - 1, j - 1)$  is not.

**Path traversal.** We start with a path along the left and top edge of the 2-filtration,  $(0, 0) \dots (0, n) \dots (n, n)$ . The filtration that we get from this path is the same as if we sorted all the simplices by the first coordinate of the left-most grades in their appearance curves. We compute persistence  $\mathbf{R} = \mathbf{DV}$  for this filtration. To simplify exposition, for every unpaired simplex  $\sigma$ , we add an implicit negative cell  $\hat{\sigma}$  at grade  $(n + 1, n + 1)$ , with  $\mathbf{R}[\hat{\sigma}] = \mathbf{D}[\hat{\sigma}] = \sigma$  and  $\mathbf{V}[\hat{\sigma}] = \hat{\sigma}$ .

We sweep through the paths of the following form,  $(0, 0) \dots (i - 1, 0) \dots (i - 1, j), (i, j) \dots (i, n) \dots (n, n)$ , transitioning one square at a time, by replacing  $(i - 1, j - 1), (i - 1, j), (i, j)$  with  $(i - 1, j - 1), (i, j - 1), (i, j)$ ; see Figure 3. As we perform such elementary steps, we build up the birth curves and report all the non-zero intervals in the diagram whose upper endpoint is in grade  $(i, j)$ , i.e., all  $\mathbf{DgmF}[\cdot, (i, j)] \neq 0$ .

**Invariant.** We maintain the following invariant, necessary to verify the correctness of each step and the running time claim. We emphasize in Section 5.1 the key parts of the matrix updates that maintain it.

1. Each negative simplex  $\tau$  along the current path (in the sense of Figure 3) maintains a birth curve, stored as a set of grades that represent its lower corners (by definition,

all are below the grade of  $\tau$ 's appearance along the path). For each lower corner  $\mathbf{a}$ , we maintain three chains,  $\mathbf{R}[\tau], \mathbf{V}[\tau], \mathbf{V}[\sigma]$ , such that  $\mathbf{R}[\tau]$  and  $\mathbf{V}[\sigma]$  are cycles that appear in the complex  $F(\mathbf{a})$ , but not in any complex  $F(\mathbf{a}')$  with  $\mathbf{a}' < \mathbf{a}$ , and  $\mathbf{R}[\tau] = \mathbf{D} \cdot \mathbf{V}[\tau]$ .

2. Any path that reaches the current grade  $(\mathbf{i}, \mathbf{j})$  and then proceeds to grade  $(\mathbf{i}, \mathbf{n})$  and then  $(\mathbf{n}, \mathbf{n})$  induces a 1-filtration. Assembling the columns  $\mathbf{R}[\tau], \mathbf{V}[\tau], \mathbf{R}[\sigma] = 0, \mathbf{V}[\sigma]$  that are stored at the lower corners below<sup>2</sup> the grades at which the path enters the upsets of the birth curves — ordering all such columns with respect to the path — we get decomposition  $\mathbf{R} = \mathbf{D}\mathbf{V}$  that satisfies the reduction assumptions ( $\mathbf{R}$  is reduced,  $\mathbf{V}$  is invertible upper-triangular).
3. If for a set of simplices along a path,  $\dots \sigma \dots \tau \dots \alpha \dots \beta \dots$ , the pairing is neither nested nor disjoint —  $\sigma$  paired with  $\alpha$ , and  $\tau$  paired with  $\beta$  — we ensure that  $\mathbf{V}[\alpha, \beta] = 0$ . (This condition is satisfied by the original algorithm [13], and although the prior work [11, 24] does not deliberately maintain this property, we explain in Appendix A the necessary extra update, and call it out in the text accompanying Figure 4.)

## 5.1 Updates

As we update the path, shifting it around the square  $(\mathbf{i}, \mathbf{j})$ , suppose only one new simplex,  $\sigma$ , appears between grades  $(\mathbf{i} - 1, \mathbf{j} - 1)$  and  $(\mathbf{i}, \mathbf{j})$ . The analysis of the previous section implies that the diagram can have a non-zero entry for  $\mathbf{DgmF}[\cdot, (\mathbf{i}, \mathbf{j})]$  or  $\mathbf{DgmF}[(\mathbf{i}, \mathbf{j}), \cdot]$  only if  $(\mathbf{i}, \mathbf{j})$  is the lower or upper corner of the appearance curve of  $\sigma$ . (Otherwise, either  $\mathbf{B} = 0$  or  $\mathbf{D} = 0$  in Theorem 4.5.)

If  $\sigma$  is positive, we add  $(\mathbf{i}, \mathbf{j})$  as a lower or upper corner of its pair's birth curve. If  $\sigma$  is negative, then for any grade  $(\mathbf{k}, \mathbf{l}) < (\mathbf{i}, \mathbf{j})$  such that  $(\mathbf{k}, \mathbf{l})$  is in the upset of the birth curve  $\text{birth}(\sigma)$ , but  $(\mathbf{k} - 1, \mathbf{l} - 1)$  is not, exactly one class is born and dies at the respective grades along any path

$$\dots, (\mathbf{k} - 1, \mathbf{l} - 1), \dots, (\mathbf{k}, \mathbf{l}), \dots, (\mathbf{i} - 1, \mathbf{j} - 1), \dots, (\mathbf{i}, \mathbf{j}), \dots$$

In other words, we are exactly in the setting of Section 4.2. From the analysis after the proof of Theorem 4.5, it follows that if  $(\mathbf{i}, \mathbf{j})$  is the lower corner of the appearance curve of  $\sigma$ , then  $\mathbf{D} = +1$ ; if it is the upper corner, then  $\mathbf{D} = -1$ . Similarly, for every lower corner in the birth curve  $\text{birth}(\sigma)$ ,  $\mathbf{B} = +1$ ; for every upper corner,  $\mathbf{B} = -1$ . Accordingly, we output  $\mathbf{DgmF}[\mathbf{a}, \mathbf{b}] = \mathbf{B} \cdot \mathbf{D}$ , where  $\mathbf{b} = (\mathbf{i}, \mathbf{j})$  and  $\mathbf{a}$  is either the lower or upper corner in the birth curve.

The only remaining possibility is that two simplices,  $\sigma$  and  $\tau$ , appear as we go from grade  $(\mathbf{i} - 1, \mathbf{j} - 1)$  to grade  $(\mathbf{i}, \mathbf{j})$ . Suppose that simplex  $\sigma$  appears along the step  $(\mathbf{i} - 1, \mathbf{j} - 1) \rightarrow (\mathbf{i}, \mathbf{j} - 1)$ , and simplex  $\tau$  appears along the step  $(\mathbf{i} - 1, \mathbf{j} - 1) \rightarrow (\mathbf{i} - 1, \mathbf{j})$ . In the remainder of this section, we analyze all possible scenarios involving such  $\sigma$  and  $\tau$ .

---

<sup>2</sup>Every grade on the periphery has a unique lower corner below it.

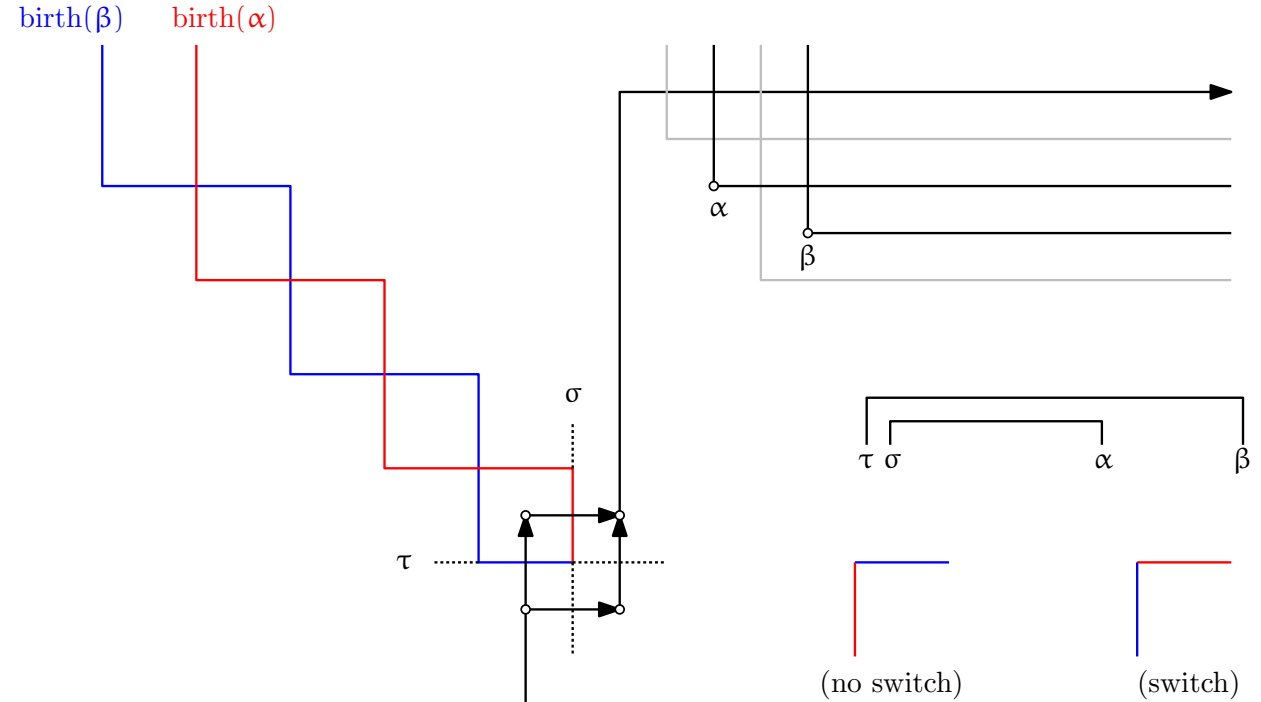


Figure 4: Positive simplices  $\sigma$  and  $\tau$ . The birth curve  $\text{birth}(\alpha)$  is shown in red; the birth curve  $\text{birth}(\beta)$ , in blue.

**$\sigma$  and  $\tau$  are both positive.** Suppose  $\sigma$  is paired with  $\alpha$ , and  $\tau$  is paired with  $\beta$ . If  $\beta$  comes first, then by Lemma 2.14 pairing of  $\sigma$  and  $\tau$  cannot switch between the two paths. It is, however, possible that the columns of  $\mathbf{R}[\alpha]$ ,  $\mathbf{V}[\alpha]$ ,  $\mathbf{V}[\sigma]$ , and  $\mathbf{R}[\beta]$ ,  $\mathbf{V}[\beta]$ ,  $\mathbf{V}[\tau]$  need to be updated. Such an update can be performed in linear time [11]; see Appendix A.

We note that the update of columns  $\mathbf{V}[\sigma]$  and  $\mathbf{V}[\tau]$  is crucial in this case. It ensures that if  $\mathbf{V}[\sigma]$  contains  $\tau$  before the transposition, then it doesn't after the transposition. This ensures correctness of Item 1 in the invariant: column  $\mathbf{V}[\sigma]$  contains only simplices present at the lower corner that stores it — a corner yet to be reached in this case.

The only way the pairing of  $\sigma$  and  $\tau$  can switch is if  $\alpha$  comes before  $\beta$ , as in Figure 4. The two paths induce the following simplex orders:  $\dots \tau \sigma \dots \alpha \dots \beta$  (before) and  $\dots \sigma \tau \dots \alpha \dots \beta$  (after). We can determine in constant time whether the pairing of  $\sigma$  and  $\tau$  switches between the two paths. Depending on the answer, we update the birth curves of  $\alpha$  and  $\beta$  in one of the two ways, shown in Figure 4. We note that if the pairing switches,  $(i, j)$  becomes a lower corner of the birth curve  $\text{birth}(\alpha)$ , and the upper corner of the birth curve  $\text{birth}(\beta)$ . We store the updated columns  $\mathbf{R}[\alpha]$ ,  $\mathbf{V}[\alpha]$ ,  $\mathbf{R}[\tau]$  with the new lower corner of  $\text{birth}(\alpha)$ .

If the pairing does not switch, and thus goes from nested to neither nested nor disjoint, it is crucial to update the column  $\mathbf{V}[\beta]$ , stored at the lower corner of  $\text{birth}(\beta)$  defined by  $\tau$ , to ensure  $\mathbf{V}[\alpha, \beta] = 0$  (necessary for Item 3 in the invariant). An example of such an update is spelled out in Case 1 in Appendix A; it takes linear time.

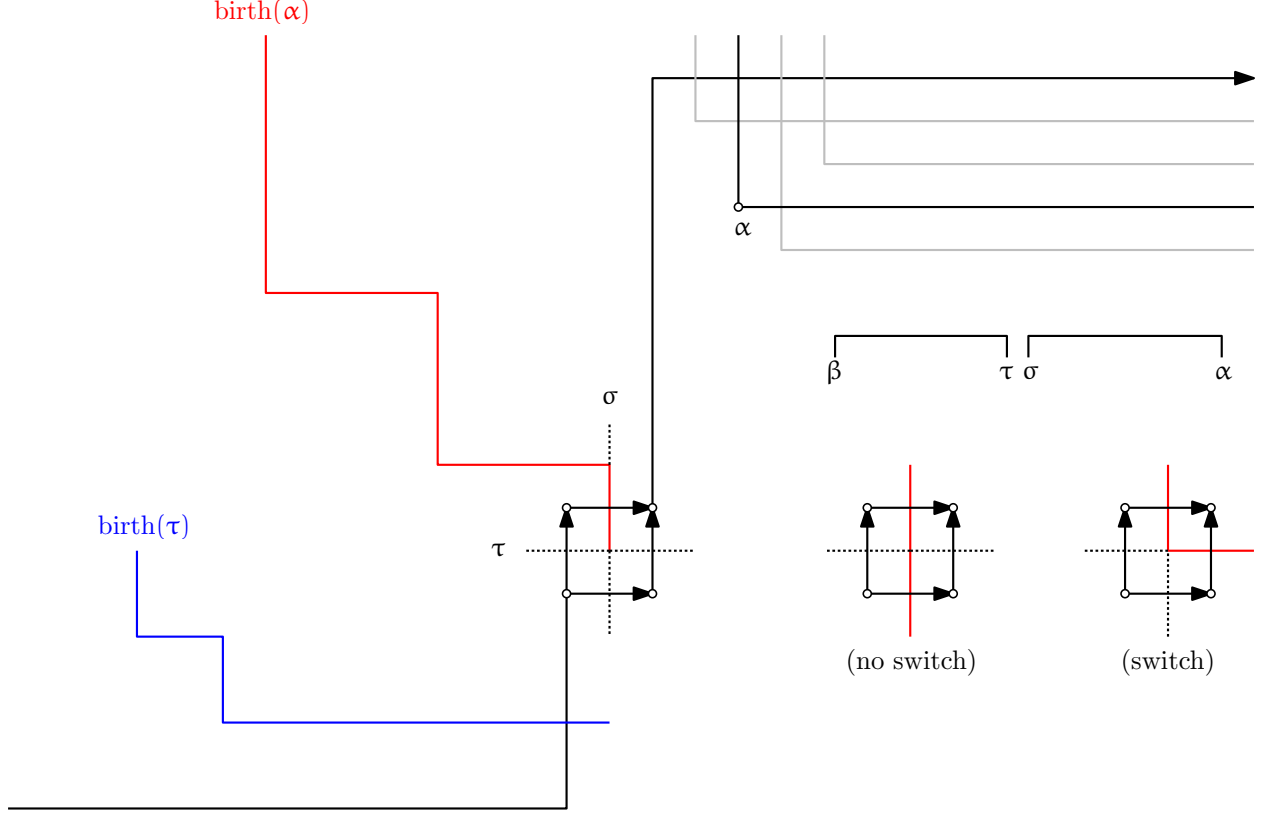


Figure 5: Positive  $\sigma$  and negative  $\tau$ . The birth curve  $\text{birth}(\alpha)$ , in red;  $\text{birth}(\tau)$ , in blue.

**$\sigma$  is positive,  $\tau$  is negative.** This scenario is illustrated in Figure 5. Consider any path that reaches grade  $(i-1, j-1)$  and then proceeds like the first path in Figure 3. Suppose it induces an ordering of simplices  $\dots \beta \dots \tau \sigma \dots \alpha$ , where  $\beta$  is paired with  $\tau$  and  $\sigma$  is paired with  $\alpha$ . We consider the path that differs by the transposition of  $\sigma$  and  $\tau$ ,  $\dots \beta \dots \sigma \tau \dots \alpha$ .

If the pairing of  $\sigma$  and  $\tau$  switches for one such path, it switches for all such paths. We can determine in constant time whether this happens. If it doesn't, there is nothing to report, and there is no need to update columns  $\mathbf{R}[\alpha]$ ,  $\mathbf{V}[\sigma]$  because  $\tau$  cannot appear in them (this follows from [11]; see Appendix A). If the pairing does switch, we update the birth curve  $\text{birth}(\alpha)$  as shown in Figure 5; grade  $(i, j)$  becomes the lower corner of the birth curve.  $\sigma$  takes over the birth curve of  $\tau$ . For every grade entering the upset of the birth curve, we are in the setting of Section 4.2. For Theorem 4.5,  $\mathbf{D} = -1$  because whichever simplex appears first going from  $(i-1, j-1)$  to  $(i, j)$  kills the respective class. For every lower corner in the birth curve,  $\mathbf{B} = +1$ ; for every upper corner,  $\mathbf{B} = -1$ . Accordingly, we output  $\text{Dgm}(\mathbf{a}, \mathbf{b}) = -1$  for all grades  $\mathbf{a}$  that are lower corners in  $\text{birth}(\sigma)$  and  $\mathbf{b} = (i, j)$ ; and  $\text{Dgm}(\mathbf{a}, \mathbf{b}) = +1$  for all  $\mathbf{a}$  that are the upper corners in  $\text{birth}(\sigma)$ .

Let us dwell for a moment on the updates to the columns of  $\mathbf{V}$ , when the pairing does switch. As explained in Appendix A (Case 3), the necessary update, encoded in matrix  $\mathbf{X}$ , subtracts a multiple  $\lambda$  of the column  $\mathbf{V}[\tau]$  from  $\mathbf{V}[\sigma]$  before the transposition (to produce

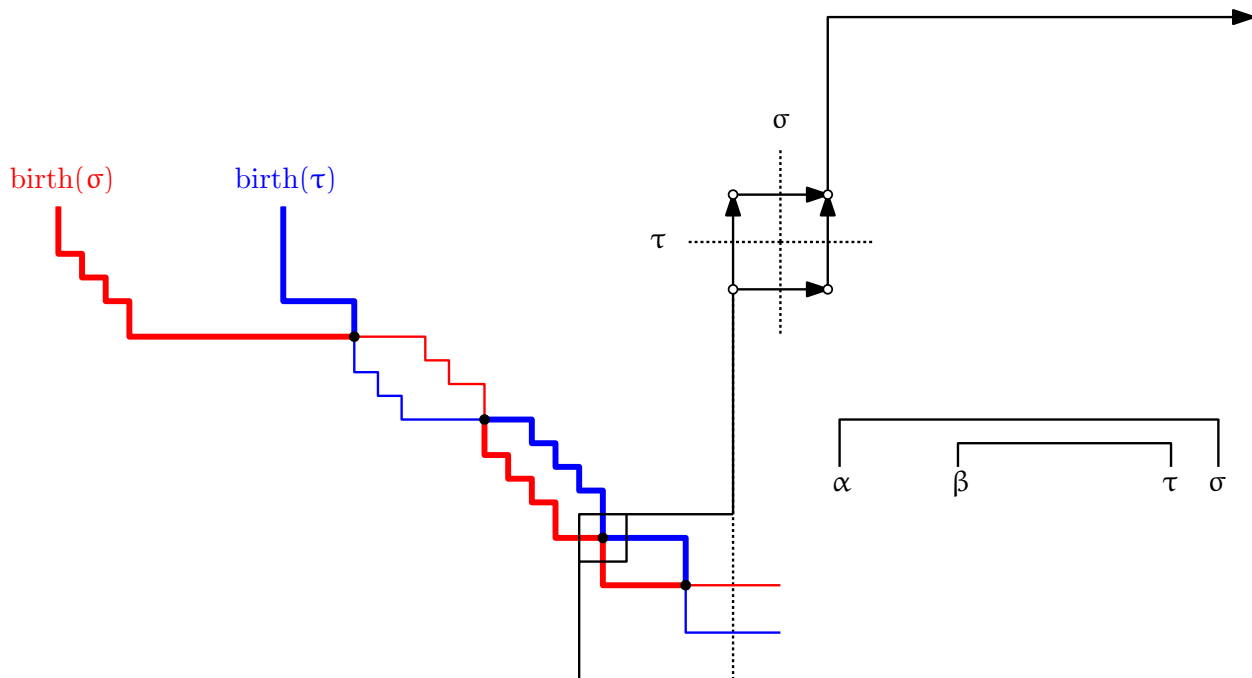


Figure 6: Negative  $\sigma$  and  $\tau$ . The birth curve  $\text{birth}(\sigma)$ , in red; the birth curve  $\text{birth}(\tau)$ , in blue.

matrix  $VX$  in Appendix A), and then adds  $(V[\sigma] - \lambda V[\tau])$  to  $\lambda V[\tau]$  (after the transposition, to produce matrix  $V' = PVXPZ$ ). In other words,  $V'[\tau] = V[\sigma]$  and  $V'[\sigma] = V[\sigma] - \lambda V[\tau]$ . The former equality means that the birth curve  $\text{birth}(\alpha)$  doesn't require any updates. But the latter equality means that for every lower corner of the birth curve  $\text{birth}(\tau)$ , we need to add  $V[\sigma]$  to  $-\lambda$  multiplied by  $V[\tau]$  stored at that corner. This update takes linear time per corner, but it's required only if the pairing switches, in which case every corner contributes to a non-zero interval in the generalized persistence diagram. We charge each such linear-time update to the output, i.e., to the  $O(Cm)$  term in the running time.

In summary, we can detect whether a switch in the pairing occurs — and if it doesn't, perform the necessary updates — in linear time. If the switch does occur, we update each step in the birth curve, but each such update corresponds to an interval in the output.

**$\sigma$  is negative,  $\tau$  is positive.** In this case, the pairing is neither nested, nor disjoint, so by Lemma 2.14 it cannot switch. But the birth curve  $\text{birth}(\sigma)$  may contain a lower corner at grade  $(\cdot, j)$ , i.e., there exists a path along which  $\tau$  and  $\sigma$  are paired. We remove this corner.

**$\sigma$  and  $\tau$  are negative.** This scenario is illustrated in Figure 6. Because both simplices are negative, each one has its own birth curve,  $\text{birth}(\sigma)$  and  $\text{birth}(\tau)$ . We can split the birth curves into two types of segments: those where the birth curve of  $\sigma$  lies below that of  $\tau$ , and vice versa. The pairing of  $\tau$  and  $\sigma$  can switch only in filtrations induced by the paths through the former (highlighted in bold in Figure 6). This follows from Lemma 2.14: only for such paths is the pairing of the two simplices nested. (Moreover, for any path through

the latter type of segment,  $V[\tau, \sigma] = 0$  — thanks to Item 3 in the invariant — so no update is necessary for these segments.)

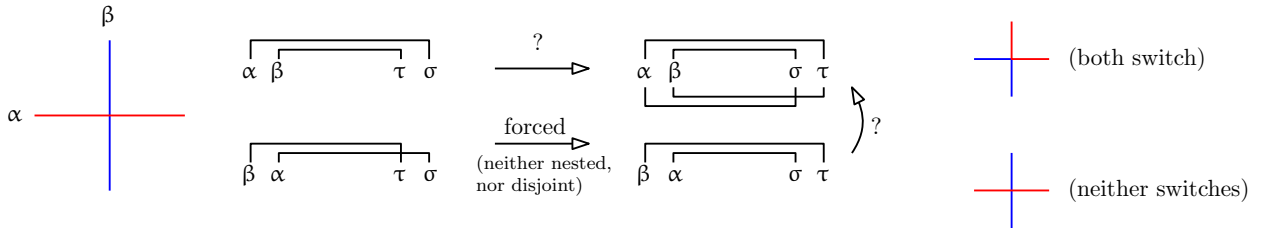
It follows from the stability of 1-dimensional persistence that if the pairing of  $\sigma$  and  $\tau$  switches for one path through the segment, it switches for all paths through the segment. Accordingly, it suffices to only check the paths around the grades, where the two birth curves intersect. We can locate all such intersections in linear time.

There are four paths around the two corners:

$$\begin{array}{cc} \dots \alpha\beta \dots \tau\sigma & \dots \alpha\beta \dots \sigma\tau \\ \dots \beta\alpha \dots \tau\sigma & \dots \beta\alpha \dots \sigma\tau \end{array}$$

We consider all combinations. In all figures, red signifies the pair of  $\sigma$  and blue, the pair of  $\tau$ .

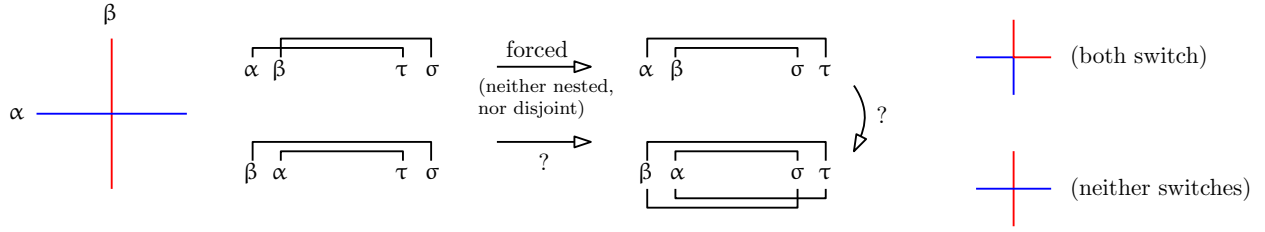
**Case A.** Suppose the pairing of the first two paths (in which  $\tau$  comes before  $\sigma$ ) is as shown in the figure. Then there are two possibilities: either the pairing switches when we transpose either pair of simplices in the top-right path,  $\dots \alpha\beta \dots \sigma\tau \dots$ , or it doesn't. We note that if it switches for one of the transpositions, it is forced to switch for both of them. If the pairing doesn't switch, it means that  $V[\tau, \sigma] = 0$  for all columns  $V[\sigma]$  stored in the birth curve  $\text{birth}(\sigma)$ , meaning there is nothing to update.



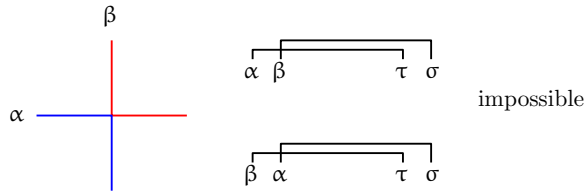
If there is a switch in the pairing, the birth curves are updated (as shown on the right of the figure) by swapping the respective segments. The update of each lower corner along the segment takes linear time, but each such corner also produces an interval in the persistence diagram. So we charge the update to the output. (We note that when updating the columns at the lower corners  $\mathbf{a} \in \text{birth}(\tau)$  of the upper birth curve, we have to choose a corner  $\mathbf{b} \in \text{birth}(\sigma)$  of the lower birth curve that lies below  $\mathbf{a}$  to perform an update. There can be multiple such choices, but any one of them works.)

The intervals reported in this case are  $\text{Dgm}[\mathbf{a}, \mathbf{b}] = +1$  for  $\mathbf{a}$  in the lower corners of  $\text{birth}(\tau)$  or the upper corners of  $\text{birth}(\sigma)$  (the corners are restricted to the appropriate segments, and the birth curve taken after the switch), and  $\text{Dgm}[\mathbf{a}, \mathbf{b}] = -1$  for  $\mathbf{a}$  in the upper corners of  $\text{birth}(\tau)$  or the lower corners of  $\text{birth}(\sigma)$ , with  $\mathbf{b} = (i, j)$ . (We note that for the lower and upper corners in the interiors of the segments, i.e., away from their intersection, these results follow from Theorem 4.5 in Section 4.2. At the intersection point, we are in the setting of Section 4.3, and the result follows from the second case in that section.)

**Case B.** This case is symmetric to Case A. That case occurs at the bottom of a segment; this case occurs at the top.



**Case C.** The pairing shown in the figure is impossible since it implies that the pairing switches for a transposition of pairs that are neither nested, nor disjoint, violating Lemma 2.14. (We note that there is no contradiction with the previous figures, since there, after the transposition,  $\sigma$  comes before  $\tau$ .)



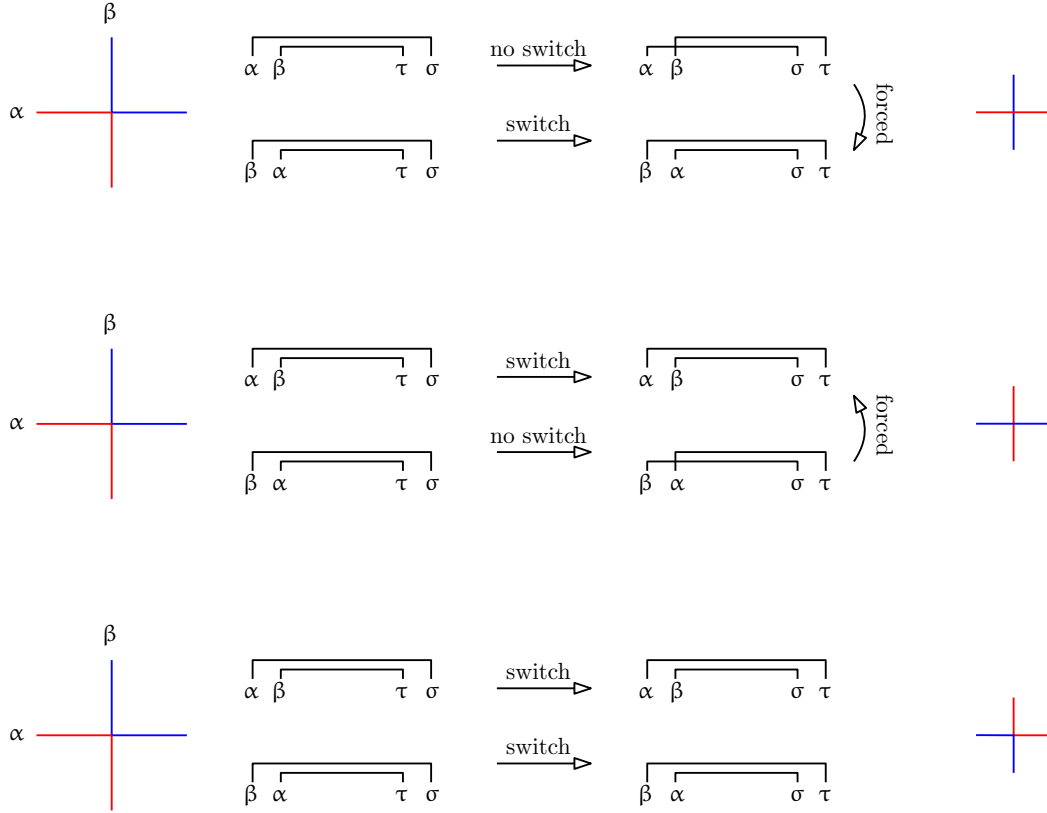
**Case D.** Suppose the pairing of the first two paths (in which  $\tau$  comes before  $\sigma$ ) is as shown in the next three figures. There are three possibilities: either the pairing switches after the transposition of  $\sigma$  and  $\tau$  in the second path, but not the first; or it switches in the first path, but not the second; or it switches in both. It's impossible for the pairing to remain the same along both paths without violating Lemma 2.14.

In the first two cases, the pairing switches for one of the two segments of the birth curves that end at the intersection point in grade  $\mathbf{b} = (i, j)$ ; in the third case, it switches for both. The segments for which the pairing does change require updates to the columns of the matrices  $\mathbf{R}$  and  $\mathbf{V}$  stored at their low corners, but each such corner also results in an interval in the diagram, and we charge the update to the output. For the segments where the pairing doesn't switch, we have  $V[\tau, \sigma] = 0$  for all columns  $V[\sigma]$  stored in the birth curve  $\text{birth}(\sigma)$ , meaning there is nothing to update.

The intervals  $(\mathbf{a}, \mathbf{b})$ , for  $\mathbf{a}$  in the lower or upper corners of the birth curves, get  $+1$  or  $-1$  as in Cases A and B. Specifically, taking the birth curves before the pairing update, we output  $\text{Dgm}[\mathbf{a}, \mathbf{b}] = +1$  for  $\mathbf{a}$  in the lower corners of  $\text{birth}(\sigma)$  and the upper corners  $\text{birth}(\tau)$ ;  $\text{Dgm}[\mathbf{a}, \mathbf{b}] = -1$  for  $\mathbf{a}$  in the upper corners of  $\text{birth}(\sigma)$  and the lower corners  $\text{birth}(\tau)$ . (This again follows from Theorem 4.5 in Section 4.2.)

The exception is when  $\mathbf{a}$  is the grade of the intersection of the two curves, i.e., the grade depicted in the figures. Here, the analysis in Section 4.3 applies: we get  $\text{Dgm}[\mathbf{a}, \mathbf{b}] = -1$  in the first two cases, and  $\text{Dgm}[\mathbf{a}, \mathbf{b}] = -2$  in the third case.





After we perform all the updates, if the birth curve  $\text{birth}(\sigma)$  has a lower corner at grade  $(\cdot, j)$ , we remove it. (This cannot happen in the previous case of disjoint pairing.)

**Infinite intervals.** After the traversal, we output the “infinite” intervals  $\text{Dgm}[\mathbf{a}, (\mathbf{n}, \mathbf{n})] = +1$  and  $\text{Dgm}[\mathbf{b}, (\mathbf{n}, \mathbf{n})] = -1$  for the lower corners  $\mathbf{a}$  and the upper corners  $\mathbf{b}$  in the birth curves of the implicit cells  $\hat{\sigma}$ .

## 5.2 Analysis

After the initial  $O(m^3)$  persistence computation, the algorithm takes  $O(n^2)$  steps. Each step requires an  $O(m)$  update, plus an update of the birth curves that we charged to the output:  $O(m)$  time for each one of the  $C$  intervals in the output. The total running time is in  $O(n^2m + Cm)$ . It is immediate from the algorithm that the size of the output  $C$  is in  $O(n^3)$ , making the whole algorithm no worse than  $O(n^4)$  brute-force approach. On the other hand,  $C$  can be as low as  $n$ : for example, if the entire 2-filtration is totally nested, i.e., if the grades of every pair of simplices are comparable in the poset.

## 6 Conclusion

Generalized persistence diagrams are a promising direction for TDA research. They generalize all the desirable properties of 1-parameter persistence used in applications. Their structure offers the possibility of following the 1-parameter blueprint, including straightforward adaptation of the newer methodologies, such as vectorizing persistence diagrams for use in machine learning [9, 28] or modifying the input data by back-propagating gradients through persistence diagrams [22, 25].

Until now, the crucial missing piece was efficient computation. We hope that the output-sensitive algorithm presented in this paper will pave the way for using generalized persistence diagrams in applications.

## References

- [1] Hideto Asashiba, Emerson G. Escolar, Ken Nakashima, and Michio Yoshiwaki. On approximation of 2d persistence modules by interval-decomposables. 2019, arXiv:1911.01637.
- [2] Paul Bendich, Herbert Edelsbrunner, Dmitriy Morozov, and Amit Patel. Homology and robustness of level and interlevel sets. *Homology, Homotopy and Applications*, 15(1):51–72, 2013.
- [3] Leo Betthauser, Peter Bubenik, and Parker B. Edwards. Graded persistence diagrams and persistence landscapes. *Discrete Comput. Geom.*, 67(1):203–230, January 2022.
- [4] Magnus Bakke Botnan, Vadim Lebovici, and Steve Oudot. On rectangle-decomposable 2-parameter persistence modules, February 2020, 2002.08894.
- [5] Magnus Bakke Botnan, Steffen Oppermann, and Steve Oudot. Signed barcodes for multi-parameter persistence via rank decompositions and rank-exact resolutions. 2021, arXiv:2107.06800.
- [6] Peter Bubenik. Statistical topological data analysis using persistence landscapes. *Journal of machine learning research: JMLR*, 16(1):77–102, 2015.
- [7] Gunnar Carlsson and Vin de Silva. Zigzag persistence. *Foundations of computational mathematics*, 10(4):367–405, August 2010.
- [8] Gunnar Carlsson and Afra Zomorodian. The theory of multidimensional persistence. *Discrete & computational geometry*, 42(1):71–93, July 2009.
- [9] Mathieu Carriere, Frederic Chazal, Yuichi Ike, Theo Lacombe, Martin Royer, and Yuhei Umeda. PersLay: A neural network layer for persistence diagrams and new graph topological signatures. *Stat*, 1050:17, 2019.

- [10] David Cohen-Steiner, Herbert Edelsbrunner, and John Harer. Stability of persistence diagrams. *Discrete & computational geometry*, 37:103–120, 2007.
- [11] David Cohen-Steiner, Herbert Edelsbrunner, and Dmitriy Morozov. Vines and vineyards by updating persistence in linear time. In *Proceedings of the Twenty-second Annual Symposium on Computational Geometry*, SCG '06, pages 119–126, New York, NY, USA, 2006. ACM.
- [12] Tamal K Dey and Cheng Xin. Generalized persistence algorithm for decomposing multi-parameter persistence modules. 2019, arXiv:1904.03766.
- [13] Herbert Edelsbrunner, David Letscher, and Afra Zomorodian. Topological persistence and simplification. *Discrete & computational geometry*, 28(4):511–533, November 2002.
- [14] Herbert Edelsbrunner, Dmitriy Morozov, and Amit Patel. Quantifying transversality by measuring the robustness of intersections. *Foundations of Computational Mathematics*, 11(3):345–361, June 2011.
- [15] Patrizio Frosini and Claudia Landi. Size theory as a topological tool for computer vision. *Pattern Recognition and Image Analysis*, 9:596–603, 11 2001.
- [16] Aziz Burak Gülen and Alexander McCleary. Galois connections in persistent homology. 2022, arXiv:2201.06650.
- [17] Gregory Henselman and Robert Ghrist. Matroid Filtrations and Computational Persistent Homology. Jun 2016, arXiv:1606.00199.
- [18] Gregory Henselman-Petrusek. Matroids and Canonical Forms: Theory and Applications. 2017, arXiv:1710.06084.
- [19] Michael Kerber and Alexander Rolle. Fast minimal presentations of bi-graded persistence modules. In *2021 Proceedings of the Workshop on Algorithm Engineering and Experiments (ALENEX)*, pages 207–220. Society for Industrial and Applied Mathematics, Philadelphia, PA, January 2021.
- [20] Woojin Kim and Facundo Mémoli. Generalized persistence diagrams for persistence modules over posets. *Journal of Applied and Computational Topology*, 5(4):533–581, 2021.
- [21] Michael Lesnick and Matthew Wright. Computing minimal presentations and bigraded betti numbers of 2-parameter persistent homology. 2019, arXiv:1902.05708.
- [22] Jacob Leygonie, Steve Oudot, and Ulrike Tillmann. A framework for differential calculus on persistence barcodes. *Foundations of computational mathematics*, 22(4):1069–1131, August 2022.

- [23] Alexander McCleary and Amit Patel. Edit distance and persistence diagrams over lattices. *SIAM Journal on Applied Algebra and Geometry*, 6(2):134–155, 2022.
- [24] Dmitriy Morozov. *Homological illusions of persistence and stability*. PhD thesis, Duke University, Durham, NC, 2008.
- [25] Arnur Nigmatov and Dmitriy Morozov. Topological optimization with big steps. 2022, arXiv:2203.16748.
- [26] Amit Patel. Generalized persistence diagrams. *Journal of Applied and Computational Topology*, 1(3):397–419, June 2018.
- [27] Amit Patel and Tatum Rask. Poincaré duality for generalized persistence diagrams of (co)filtrations. 2022, arXiv:2212.14610.
- [28] Jose A Perea, Elizabeth Munch, and Firas A Khasawneh. Approximating continuous functions on persistence diagrams using template functions. *Foundations of computational mathematics*, June 2022.
- [29] Gian-Carlo Rota. On the foundations of combinatorial theory I. Theory of Möbius Functions. *Zeitschrift für Wahrscheinlichkeitstheorie und Verwandte Gebiete*, 2(4):340–368, 1964.
- [30] Richard P. Stanley. *Enumerative Combinatorics: Volume 1*. Cambridge University Press, USA, 2nd edition, 2011.
- [31] Oliver Vipond. Multiparameter persistence landscapes. *Journal of machine learning research: JMLR*, 21:61–61, 2020.
- [32] Afra Zomorodian and Gunnar Carlsson. Computing persistent homology. *Discrete & computational geometry*, 33(2):249–274, February 2005.

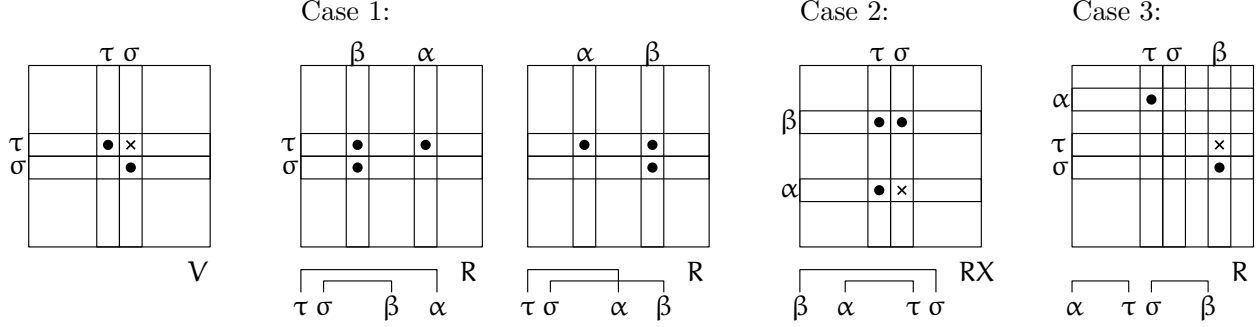


Figure 7: Updates of the matrices  $R$  and  $V$  after the transposition of two simplices.

## A Transposition Analysis

The updates to 1-dimensional persistence when two consecutive simplices,  $\tau$  and  $\sigma$ , transpose are studied in [11, 24]. Given a boundary matrix  $D$  of a filtration, together with its decomposition  $R = DV$  into a reduced matrix  $R$  and an invertible upper-triangular matrix  $V$ , let  $P$  denote the permutation matrix that transposes two adjacent columns (if multiplied on the right) or rows (if multiplied on the left) that correspond to the simplices  $\tau$  and  $\sigma$ . We are interested in finding the decomposition  $R' = (PDP)V'$ , where  $R'$  is reduced and  $V'$  is invertible upper-triangular.

**Matrix  $V$  update.** The only way in which  $V' = PVP$  can fail to satisfy this condition is if  $V[\tau, \sigma] \neq 0$ . If this is the case, we denote by  $X$  the matrix that subtracts an appropriate multiple  $\lambda$  of column  $V[\cdot, \tau]$  from column  $V[\cdot, \sigma]$  to make  $V[\tau, \sigma] = 0$ . In this case, matrix  $PVXP$  is invertible upper-triangular. We abuse the notation, and let  $X$  denote either this update matrix, or identity if no update was required.

**Case 1.** Suppose both simplices  $\tau$  and  $\sigma$  are positive, paired with simplices  $\alpha$  and  $\beta$  respectively. (The case where either one of the simplices is unpaired is analogous.) In this case, it's possible that columns  $R[\cdot, \alpha]$  and  $R[\cdot, \beta]$  are such that  $PRXP$  is not reduced. This happens when  $R[\tau, \beta] \neq 0$ ; see Figure 7. If this happens, we can subtract an appropriate multiple of the first of these two columns from the second, to ensure that the new matrix is reduced. Denoting this subtraction with matrix  $Y$ , we get decomposition  $(PRXPY) = (PDP)(PVXPY)$ .

If the pairing was nested before the transposition, but did not switch after the transposition (and thus became neither nested, nor disjoint), i.e., if  $PRXP$  is already reduced, it is possible for the entry  $V[\beta, \alpha] \neq 0$ . The prior work [11, 24] does not pay any special attention to this case, but, in order to satisfy Item 3 in the invariant in Section 5, we need to subtract an appropriate multiple of the column  $V[\cdot, \beta]$  from the column  $V[\cdot, \alpha]$ . Denoting this update with matrix  $Y'$ , we get a decomposition  $(PRXPY') = (PDP)(PVXPY')$ . In this case, matrix  $PRXPY'$  is necessarily reduced. The pairs of any  $\alpha'$  that were added as non-zero entries  $V'[\alpha', \alpha]$  are necessarily nested in the pair  $\sigma$ - $\alpha$ .

**Case 2.** Suppose both simplices  $\tau$  and  $\sigma$  are negative, paired with simplices  $\alpha$  and  $\beta$  respectively. In this case, if  $\alpha$  comes after  $\beta$ , then the columns  $(\text{PRXP})[\cdot, \tau]$  and  $(\text{PRXP})[\cdot, \sigma]$  may not be reduced because of the update caused by matrix  $\mathbf{X}$ ; see Figure 7. In this case, we can apply matrix  $\mathbf{Z}$  after the transposition. This matrix replaces the later column (of simplex  $\tau$  after the transposition) by multiplying it by  $\lambda$  and adding an earlier column. In other words, we get

$$\begin{aligned} (\text{PRXPZ})[\cdot, \tau] &= (\text{PRXP})[\cdot, \sigma] + \lambda(\text{PRXP})[\cdot, \tau] \\ &= ((\text{PRP})[\cdot, \sigma] - \lambda(\text{PRP})[\cdot, \tau]) + \lambda(\text{PRP})[\cdot, \tau] \\ &= (\text{PRP})[\cdot, \sigma]. \end{aligned}$$

(The same analysis applies to  $(\text{PVXPZ})[\cdot, \tau]$ .) In other words, the second of the two columns in matrices  $\mathbf{R}$  and  $\mathbf{V}$  do not change. The resulting matrix is reduced and the decomposition,  $(\text{PRXPZ}) = (\text{PDP})(\text{PVXPZ})$ , satisfies the two conditions.

If the pairing went from nested to neither nested nor disjoint (i.e., it did not switch), the original update  $\mathbf{X}$  to matrix  $\mathbf{V}$  ensures that Item 3 in the invariant in Section 5 is satisfied.

**Case 3.** Suppose simplex  $\tau$  is negative, while simplex  $\sigma$  is positive; again the two are paired with  $\alpha$  and  $\beta$  respectively. If matrix  $\mathbf{V}$  required an update, then because the column  $\mathbf{R}[\cdot, \sigma] = 0$ , the columns  $\tau$  and  $\sigma$  in matrix  $(\text{PRXP})$  are the same, up to the factor of  $-\lambda$ , requiring a further reduction by an application of matrix  $\mathbf{Z}$  from Case 2. We get decomposition,  $(\text{PRXPZ}) = (\text{PDP})(\text{PVXPZ})$ . We note that it is not immediately obvious, but true that  $\mathbf{R}[\tau, \beta] \neq 0$  iff  $\mathbf{V}[\tau, \sigma] \neq 0$ .

## B Algorithm Summary

---

### Algorithm 1: High-level overview

---

- 1 compute 1-parameter persistence  $\mathbf{R} = \mathbf{D}\mathbf{V}$ , simplices sorted by the lowest  $x$ -coordinate,  $x(\sigma)$ , in their appearance curve
  - 2 **foreach** *positive*  $\sigma$  **do**
  - 3     **if**  $\sigma$  *is paired with*  $\tau$  **then**
  - 4         |      $\text{birth}(\tau) = ((\mathbf{R}[\tau], \mathbf{V}[\tau], \mathbf{V}[\sigma], (x(\sigma), \mathbf{n})))$
  - 5     **else if**  $\sigma$  *is unpaired* **then**
  - 6         |     pair  $\sigma$  with  $\hat{\sigma}$  implicitly added at grade  $(\mathbf{n} + 1, \mathbf{n} + 1)$
  - 7         |      $\text{birth}(\hat{\sigma}) = ((\mathbf{R}[\hat{\sigma}] = \sigma, \mathbf{V}[\hat{\sigma}] = \hat{\sigma}, \mathbf{V}[\sigma], (x(\sigma), \mathbf{n})))$
-

---

```

8 for  $i = 1$  to  $n$  do
9   for  $j = n$  to  $1$  do
10    if  $(i, j)$  is the lower-corner in the appearance curve of some  $\sigma$  then
11     if  $\sigma$  is positive, paired with  $\tau$  then
12      set the  $y$ -coordinate of the last corner in  $\text{birth}(\tau)$  to  $j$ 
13     else if  $\sigma$  is negative then
14      output  $(+1, \mathbf{a}, (i, j))$  for  $\mathbf{a} \in \mathbf{l}(\text{birth}(\sigma))$ 
15      output  $(-1, \mathbf{a}, (i, j))$  for  $\mathbf{a} \in \mathbf{u}(\text{birth}(\sigma))$ 
16    else if  $(i, j)$  is the upper-corner in the appearance curve of some  $\sigma$  then
17     if  $\sigma$  is positive, paired with  $\tau$  then
18      make a copy of the last corner in  $\text{birth}(\tau)$ , setting its grade to  $(i, j)$ 
19      (component  $j$  will be updated later)
20     else if  $\sigma$  is negative then
21      output  $(-1, \mathbf{a}, (i, j))$  for  $\mathbf{a} \in \mathbf{l}(\text{birth}(\sigma))$ 
22      output  $(+1, \mathbf{a}, (i, j))$  for  $\mathbf{a} \in \mathbf{u}(\text{birth}(\sigma))$ 
23    else if  $(i, j)$  is the grade where  $\sigma$  and  $\tau$  appear together for the first time
24     then
25     if  $\tau$  and  $\sigma$  are positive then
26      let  $\alpha$  be the pair of  $\sigma$  and  $\beta$ , the pair of  $\tau$ 
27      update the birth curve and  $\mathbf{R}[\alpha]$ ,  $\mathbf{V}[\alpha]$ ,  $\mathbf{V}[\sigma]$ ,  $\mathbf{R}[\beta]$ ,  $\mathbf{V}[\beta]$ ,  $\mathbf{V}[\tau]$  as
28      described in the text accompanying Figure 4
29     else if  $\tau$  is negative,  $\sigma$  is positive then
30      let  $\alpha$  be the pair of  $\sigma$ 
31      determine if the pairing switches (text accompanying Figure 5),
32      extend  $\text{birth}(\alpha)$  accordingly
33     if the pairing switches then
34       $\text{birth}(\sigma)$  takes over  $\text{birth}(\tau)$ 
35      update the columns stored at the corners of  $\text{birth}(\sigma)$ 
36      output  $(-1, \mathbf{a}, (i, j))$  for  $\mathbf{a} \in \mathbf{l}(\text{birth}(\sigma))$ 
37      output  $(+1, \mathbf{a}, (i, j))$  for  $\mathbf{a} \in \mathbf{u}(\text{birth}(\sigma))$ 
38     else if  $\tau$  and  $\sigma$  are negative then
39      identify distinct segments of the birth curves  $\text{birth}(\tau)$ ,  $\text{birth}(\sigma)$ 
40     foreach segment do
41      determine if the pairing switches
42      update and output as described in the text accompanying Figure 6
43     if the first corner in  $\text{birth}(\sigma)$  is  $(\cdot, j)$  then remove it
44     else if  $\tau$  is positive,  $\sigma$  is negative then
45     if the first corner in  $\text{birth}(\sigma)$  is  $(\cdot, j)$  then remove it
46  foreach  $\hat{\sigma}$  added in Line 6 do
47   output  $(+1, \mathbf{a}, (n, n))$  for  $\mathbf{a} \in \mathbf{l}(\text{birth}(\hat{\sigma}))$ 
48   output  $(-1, \mathbf{a}, (n, n))$  for  $\mathbf{a} \in \mathbf{u}(\text{birth}(\hat{\sigma}))$ 

```

---